Sensor and Simulation Notes

Note 408

July 1997

Coaxial Beam-Rotating Antenna (COBRA) Prototype Measurements

Clifton C. Courtney, David Slemp and Darren Baum
Voss Scientific

Carl E. Baum, Robert Torres and William Prather
Phillips Laboratory / WSQW

Abstract

An azimuthally symmetric mode, typical of the output mode of many high power microwave (HPM) sources, radiates a characteristic low gain pattern with a boresight null. The Coaxial Beam-Rotating Antenna (COBRA) is designed to be driven by an azimuthally symmetric mode such as the TM_{01} circular waveguide or TEM coaxial mode, and will radiate a high gain, boresight peak pattern with circular polarization. The theory of the COBRA has been presented in an earlier note, and this note describes the results of low-power experiments of an X-band COBRA prototype which has recently been fabricated. The experiments were meant to measure the electromagnetic characteristics of its radiated field, the physical aspects of the COBRA prototype are also described. The radiated far-field absolute gain patterns (in one or more of the principal planes) for N = 1, 2 and 4 COBRA configurations, and the phase relations between the orthogonal polarizations on boresight were measured. The experimental procedure is described, and detailed graphs of the results are presented. A number of tables which summarize the radiating properties of the prototype antenna are also provided.

Table of Contents

1. INTRODUCTION 7
2. COBRA PROTOTYPE ANTENNA DESCRIPTION 8
3. MEASUREMENT SYSTEM CHARACTERISTICS 10
   3.1 Antenna Measurement System Overview 10
   3.2 Narrowband Antenna Measurement System Sensor Characteristics 11
      3.2.1 Transmit (TX) Antenna 11
      3.2.2 Reference (REF) Antenna 12
      3.2.3 Calibration (CAL) Antenna 17
4. CIRCULAR WAVEGUIDE FEED HORN CHARACTERISTICS 22
   4.1 Circular Waveguide VSWR 22
   4.2 Circular Waveguide Feed Horn Pattern 24
5. N = 1 COBRA MEASUREMENTS 26
   5.1 Focal Point Adjustment Measurements 26
   5.2 Horizontal Polarization Azimuthal Pattern 26
   5.3 Vertical Polarization Azimuthal Pattern 27
   5.4 Frequency Dependence of the N=1 COBRA 27
6. N=2 COBRA MEASUREMENTS 30
   6.1 Cross-Polarization Pattern 30
   6.2 Co-Polarized Pattern 31
   6.3 Frequency Dependence of the Co-Polarized Azimuthal Pattern 31
   6.4 Alternate Co-Polarized Pattern 32
7. N=4 COBRA MEASUREMENTS 37
   7.1 N=4 : Tx Horn = Horizontal Polarization 37
   7.2 N=4 : TX Horn = Vertical Polarization 38
   7.3 Frequency Dependence of the Azimuthal Pattern 38
   7.4 Boresight Phase Relations 38
      7.4.1 Circular Polarization Measurement Procedure 39
      7.4.2 Circular Polarization Measurement Results 40
8. SUMMARY, OBSERVATIONS AND CONCLUSIONS 47
   8.1 Physical Aperture of the COBRA Prototype 47
   8.2 Performance Summary of the COBRA Prototype 47
   8.3 Conclusions and Observations 48
9. REFERENCES 49

Table of Figures

Figure 2-1 The prototype COBRA antenna. It is a parabolic reflector partitioned into 4 sectors and fed by a conical horn located at the focal point....8

Figure 3-1 Functional block diagram of the Narrowband Antenna Measurement system. 11

Figure 3-2 Power loss due to impedance mismatch, as a function of frequency, of the dual-ridged waveguide horn (AEL-1498). This horn was used as one of the TX, REF and / or CAL antennas....13

Figure 3-3 Measured gain across the bandwidth of the AEL 1498 dual-ridged waveguide horn. This curve became part of the calibration record of the antenna measurement system....13

Figure 3-4 Cross-polarized gain of the AEL 1498 dual-ridged waveguide horn. 14

Figure 3-5 Polar pattern of co-polarized component (horizontally polarized) of the AEL 1498 dual-ridged waveguide horn antenna radiated field. The pattern was measured at an operating frequency of 10 GHz....15

Figure 3-6 Polar pattern of co-polarized component (vertically polarized) of the AEL 1498 dual-ridged waveguide horn antenna radiated field at 10 GHz....16

Figure 3-7 Power loss due to impedance mismatch, as a function of frequency, of the X-band standard-gain horn antenna. This horn was used as one of the TX, REF and / or CAL antennas. 18

Figure 3-8 Measured gain as a function of frequency of the X-band standard-gain horn antenna. This curve became part of the calibration record of the antenna measurement system....18

Figure 3-9 Measured cross-polarized gain of the dual-ridged waveguide horn at 10 GHz. These values are somewhat pessimistic, the literature reports cross-polarization ratios of about 50 dB! 19

Figure 3-10 Polar pattern of co-polarized component (horizontally polarized) of the radiated field of the X-band standard-gain horn antenna at 10 GHz. 20

Figure 3-11 Polar pattern of co-polarized component (vertically polarized) of the radiated field of the X-band standard-gain horn antenna at 10 GHz. 21

Figure 4-1 Input VSWR, as a function of frequency, of the COBRA prototype feed horn. The feed horn was tuned nominally to 10 GHz....23

Figure 4-2 Power loss, as a function of frequency, due to impedance mismatch of the COBRA prototype feed horn. Note the response reflects the waveguide cutoff at about 8.5 GHz....23

Figure 4-3 Co-polarized pattern of the COBRA prototype feed horn in the azimuthal plane. The pattern was measured at 10 GHz. 25
Figure 4-4 Cross-polarized pattern of the COBRA prototype feed horn in the azimuthal plane at 10 GHz. 25
Figure 5-1 Focal length dependence of the co-polarized pattern, in the azimuthal plane of the N=1 COBRA prototype. 28
Figure 5-2 Co-polarized azimuthal pattern of the N=1 COBRA prototype at 10 GHz. 28
Figure 5-3 Co-polarized azimuthal patterns for several frequencies (9, 10, 11, 12 GHz) of the N=1 COBRA prototype. 29
Figure 6-1 Cross-polarized pattern of the N=2 COBRA prototype in the azimuthal plane. The measurement frequency was 10 GHz. 33
Figure 6-2 Co-polarized pattern of the N=2 COBRA prototype in the azimuthal plane at 10 GHz. 33
Figure 6-3 Co-polarized pattern of the N=2 COBRA prototype in the azimuthal plane. The measurement frequency was 9 GHz. 34
Figure 6-4 Co-polarized pattern of the N=2 COBRA prototype in the azimuthal plane. The measurement frequency was 9.5 GHz. 34
Figure 6-5 Co-polarized pattern of the N=2 COBRA prototype in the azimuthal plane. The measurement frequency was 10 GHz. This measurement is independent of the measurement depicted in Figure 6-2. 35
Figure 6-6 Co-polarized pattern of the N=2 COBRA prototype in the azimuthal plane. The measurement frequency was 10.5 GHz. 35
Figure 6-7 Co-polarized pattern of the N=2 COBRA prototype in the azimuthal plane. The measurement frequency was 11 GHz. 36
Figure 6-8 Co-polarized pattern of the N=2 COBRA prototype in the elevation plane. The measurement frequency was 10 GHz. 36
Figure 7-1 Co-polarized pattern of the N=4 COBRA prototype in the elevation plane. The measurement frequency was 10 GHz. 41
Figure 7-2 Co-polarized pattern of the N=4 COBRA prototype in the azimuthal plane. The measurement frequency was 10 GHz. 41
Figure 7-3 Co-polarized pattern of the N=4 COBRA prototype in the azimuthal plane. The measurement frequency was 9 GHz. 42
Figure 7-4 Co-polarized pattern of the N=4 COBRA prototype in the azimuthal plane. The measurement frequency was 9.5 GHz. 42
Figure 7-5 Co-polarized pattern of the N=4 COBRA prototype in the azimuthal plane. The measurement frequency was 10 GHz. 43

Figure 7-6 Co-polarized pattern of the N=4 COBRA prototype in the azimuthal plane. The measurement frequency was 10.5 GHz. 43
Figure 7-7 Co-polarized pattern of the N=4 COBRA prototype in the azimuthal plane. The measurement frequency was 11 GHz. 44
Figure 7-8 Relative magnitude of the horizontal polarized component of the boresight field of the N=4 COBRA as a function of frequency. 44
Figure 7-9 Relative magnitude of the vertical polarized component of the boresight field of the N=4 COBRA as a function of frequency. 45
Figure 7-10 Relative phase of the horizontal polarized component of the boresight field of the N=4 COBRA as a function of frequency. 45
Figure 7-11 Relative phase of the vertical polarized component of the boresight field of the N=4 COBRA as a function of frequency. 46

List of Tables

Table 4-1 A summary of the power loss values of the COBRA prototype feed horn due to mismatch as a function of frequency. 22

Table 6-1 Relative sector displacements for an N=2 COBRA configuration. 30

Table 6-2 Summary of the pattern characteristics, as a function of frequency, of an N=2 COBRA....31

Table 7-1 Relative sector displacements for an N=4 COBRA configuration. 37

Table 7-2 Summary of pattern characteristics, as a function of frequency, of an N=4 COBRA....38

Table 7-3 Summary of the boresight polarization characteristics, as a function of frequency, of an N=4 COBRA....40

Table 8-1 Physical aperture gain of the 24-inch COBRA parabolic reflector....47

Table 8-2 Performance summary for the COBRA prototype measurements....48

1. INTRODUCTION

The Coaxial Beam-Rotating Antenna (COBRA) design and engineering effort is directed toward developing antennas that can be excited with an azimuthally symmetric feed pattern, and which radiate a boresight peak pattern. Many microwave generators, including many of the most capable high power mircrowave (HPM) sources, have an output mode or field distribution that exhibits azimuthal symmetry (the coaxial TEM and circular waveguide TM_{01} modes for example). The field pattern radiated from an aperture that exhibits azimuthal field symmetry is one with a boresight null. This type of pattern is typically low gain, and very difficult to utilize in an actual mission. The COBRA geometries suggest techniques to transform an azimuthally symmetric feed illumination (either established by a guided wave, or a radiated field with azimuthal symmetry), into an aperture field distribution that produces a boresight peak in the radiated pattern. In addition, the polarization of the boresight peak is adjustable; either sense of linear polarization, as well as either sense of circular polarization, can be achieved. In fact, by slight adjustments to the geometry of the COBRA, any arbitrary elliptical polarization can be generated on boresight. The theoretical characteristics of a COBRA-type antenna are described in Phillips Laboratory Sensor and Simulation Note 395 [1].

This document describes the results of antenna gain and pattern measurements of a COBRA prototype. The antenna was designed and built as part of a Small Business Innovation for Research (SBIR) Phase I program, and the antenna characterization is one of the first tasks of the Phase II program. The objectives of the measurement program were to characterize the gain, pattern, radiated field polarization, bandwidth and efficiency characteristics of the COBRA prototype. The main tasks were to:

1. Measure the radiated pattern of the feed horn when driven by the TM_{01} circular waveguide mode;

2. Adjust and optimize the feed horn position at the focal point of the main reflecting surface;

3. Measure the N=1 COBRA pattern (both polarizations) along the main phi-pattern cut;

4. Measure the N=2 COBRA pattern (both polarizations) along the main phi-pattern cut. Physically rotate the antenna 90°, and measure the theta-pattern cut. Also, measure frequency response on either side of the nominal frequency design point (f_0 = 10 GHz);

5. Measure the N=4 COBRA pattern (both polarizations) in the main phi-pattern cut. Symmetry dictates that the theta-pattern cut should be the same, measure frequency response on either side of the frequency design point;

6. Measure the phase relation between the components of the circularly polarized N=4 COBRA pattern in the main phi-pattern cut; and

7. Measure total system efficiency, directivity, and power gain.

2. COBRA PROTOTYPE ANTENNA DESCRIPTION

Figure 2-1is a front-perspective photograph of the COBRA prototype. It is an N=4 sector design, meaning that the main parabolic reflector has been cut into four equal-angle sectors. The sectors are adjustable such that the antenna configuration can be N = 1, 2 or 4. A segmented 0.6096 m (24 inch) diameter parabolic reflector, with an F/d ratio of 0.375 (focal length = 0.2286 m, or 9 inches), comprises the main reflector of the COBRA prototype. The base of the supporting infrastructure is made of 0.635 cm (¼-inch) aluminum stock sheet, to which Unistrut elements are attached. These hold and support the antenna's individual quadrants. Two additional aluminum (Al) plates, 0.9525 cm ($^3/_8$-inch) stock, are used for mounting, translational adjustment and alignment. Three 1.27 cm ($^1/_2$-inch) diameter pins per quadrant are pressed into the lower Al plate, then passed through bushings in the upper plate. A $^7/_8$-inch stud is screwed into the bottom plate and provides vertical (translational) adjustment of the quadrant's position with the pins. The four quadrants come together at the reflector's vertex. On the reverse side, a tongue-in-groove geometry mates with an assembly bolted to each quadrant. Turnbuckles, two per quadrant, then permit rotational adjustment. Each turnbuckle has both left- and right-hand thread so rotation in one direction expands the turnbuckle, and rotation in the other direction draws it in.

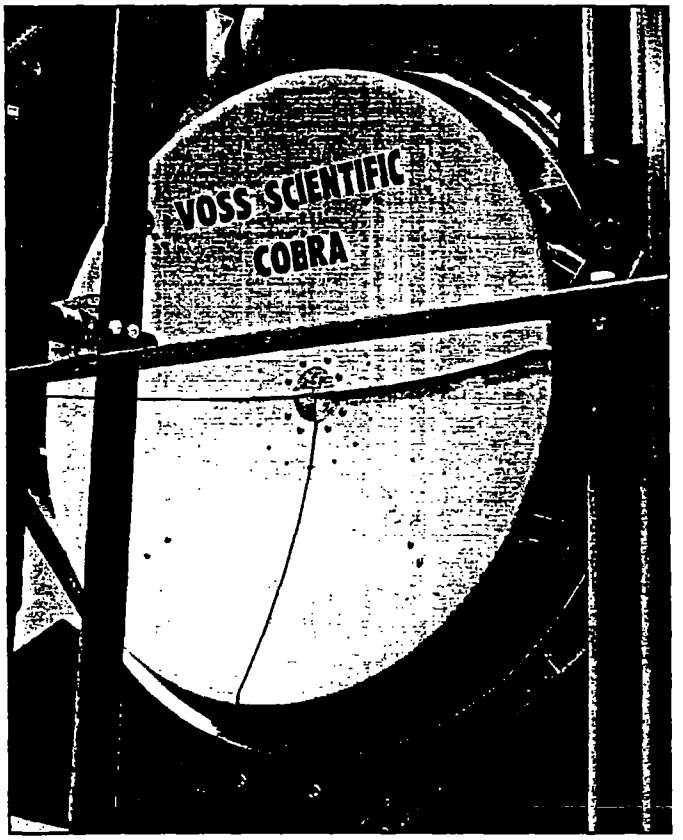

Figure 2-1. The prototype COBRA antenna. It is a parabolic reflector partitioned into 4 sectors and fed by a conical horn located at the focal point.

The following physical dimensions characterize the COBRA prototype.

weight:	100 kg (220 lbs)
dimensions:	0.9398 m x 0.9398 m x 0.762 m (37 in x 37 in x 30 in)

The feed horn is also visible in Figure 2-1. It is simply a circular waveguide (copper pipe, approx. 1.75 cm ID) driven from one end by a custom coax-to-TM_{01} mode launcher, and open at the other. The feed horn is held in place by a Plexiglas housing that permits in /out adjustment. This provides a way to match the horn's phase center to the reflector's focal point. The Plexiglas housing is bolted to a pair of thin fiberglass cross members. These cross members are slotted at the ends and attached to the Unistrut frame. The slots permit x/y adjustment of the location of the feed horn. A mode filter is resident in the circular waveguide. It helps prevent propagation to the feed horn aperture of unwanted modes that are not azimuthally symmetric.

Each of the four surface quadrants seen in the figure are positioned in a manner dictated by the COBRA antenna theory [1]. The displacement of the antenna surfaces (from the nominal position) is given by

$$\tau_n = \frac{(n-1)\lambda}{N\left[1+\cos(\theta)\right]}$$

where n = sector number, N = total number of sectors (1, 2 or 4 for the cases described here), and θ = the angle from the axis (the line from the paraboloidal vertex to the focal point) of the reflector to the position on the reflector surface. Because the prototype was built with four independently adjustable surfaces, we can first configure the antenna as an N = 1 (nominal configuration), then as N = 2 and N = 4 COBRA configurations.

3. MEASUREMENT SYSTEM CHARACTERISTICS

This section presents an overview of the antenna measurement system used to conduct measurements of the COBRA prototype. A detailed description of the system's sensors (antennas) is also given.

3.1 Antenna Measurement System Overview

The PL Narrowband Antenna Measurement System utilizes an HP 8510C Vector Network Analyzer paired with a custom s-parameter test set. It can measure antenna gain over the 0.045 - 12 GHz band, and has been custom modified to operate over long distances. Using a pair of HP microwave frequency sources, the system displays a 90-dB dynamic range, and will provide up to 20 dBm (30 dBm without lock) of radiated RF power (easily amplified to higher powers). Custom software fully automates data acquisition, reduction, analysis and archival.

The system measures the absolute gain of an antenna under test (AUT) using two independent measurements and a comparison method. A system transmit (TX) antenna radiates RF power toward a suite of co-located antennas. The first measurement records the ratio of the received power of a calibration (CAL) antenna to a reference (REF) antenna. The second measurement records the ratio of the received power of an AUT to a REF antenna. The CAL antenna is a well-characterized antenna for which the frequency response (gain) is known and recorded in the antenna range system database. The REF antenna has a broad response characteristic about the frequency bandwidth of interest. Both the REF and CAL antennas are fixed in position and orientation.

The second measurement records the AUT to REF power ratio, and the antenna range data reduction module determines the ratio of the two measurements.

$$\frac{AUT}{REF} / \frac{CAL}{REF} = \frac{AUT}{CAL}$$

The AUT gain is then determined by subtracting the known (calibrated) response, in dB, of the CAL antenna

$$AUT_{Gain} = \left(\frac{AUT}{REF}\right)_{dB} - \left(\frac{CAL}{REF}\right)_{dB} - CALGain_{dB}$$

A functional block diagram of the system is shown in Figure 3-1. The system is more complex than just described, and a full description of the system and its capabilities can be found in [2]. The characteristics of the system antennas are described in the next section.

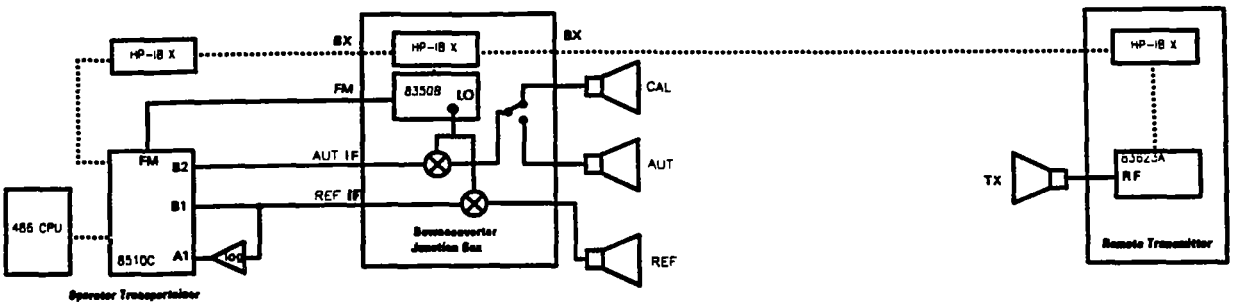

Figure 3-1 Functional block diagram of the Narrowband Antenna Measurement system.

3.2 Narrowband Antenna Measurement System Sensor Characteristics

Four antennas (sensors) are typically associated with the Narrowband Antenna Measurement System. They are:

1. Antenna Under Test (AUT)—The antenna to be characterized in terms of its spatial pattern and frequency dependence.
2. Reference Antenna (REF)—The "port-two" antenna, common in both measurements needed to determine the AUT gain.
3. Calibration Antenna (CAL)—A well characterized antenna, its response is used to make an antenna comparison-type gain measurement of the AUT.
4. Transmit Antenna (TX) - the antenna that radiates the RF signal used in the measurements.

The input impedance as a function of frequency, the boresight gain as a function of frequency, and the azimuthal pattern of the antennas used for the TX, REF and CAL functions are given below.

3.2.1 Transmit (TX) Antenna

An AEL-1498 dual-ridged waveguide horn antenna (2 - 18 GHz) was used as the transmit antenna during the COBRA prototype measurements. This worked well for these measurements because its bandwidth covered the 9-11 GHz bandwidth of interest, and it radiated a broad pattern that equally illuminated the AUT, REF and CAL antennas. The AEL-1498's input impedance was well matched over the test bandwidth. The power rejection of the AEL 1498 was determined from measured values of the input impedance, and is given as a function of frequency in Figure 3-2. This figure is the amount of power not available for radiation due to impedance mismatch at the terminals of the antenna. Note that less than 0.2 dB of power is lost to impedance mismatch over the band of interest, and the response is fairly flat.

Figure 3-3 depicts the co-polarized boresight gain as a function of frequency of the AEL-1498. The gain is nominally 10 dBi (dBi = gain relative to isotropic) across the bandwidth of

interest. Figure 3-4 depicts the cross-polarized boresight gain as a function of frequency of the AEL-1498. The cross-polarized gain is less than -55 dBi across the bandwidth of interest. This measurement is somewhat suspect; the cross-polarized characteristics are a little too good. Typical polarization ratios (vertical transmit horn, and horizontal receive horn, or vice versa) are -50 dBi for standard gain horns. A good polarization ratio (< -20 dB) is important when measuring the COBRA prototype's two linear polarizations.

Figure 3-5 depicts the azimuthal pattern for horizontal orientation (radiated electric field parallel to the chamber floor) of the AEL-1498 antenna. A nominal boresight gain of 10 dBi is indicated, but the pattern about the boresight direction varies somewhat and shows some asymmetry. The azimuthal pattern for vertical orientation (radiated electric field perpendicular to the chamber floor) of the AEL-1498 antenna is depicted in Figure 3-6, which shows a very smooth and symmetric pattern. This could indicate that slightly more unwanted scattering is associated with measurements made with the system antennas horizontally polarized.

3.2.2 Reference (REF) Antenna

The reference (REF) antenna used during the COBRA prototype measurements was an AEL-1498 dual-ridged waveguide antenna. The characteristics of the AEL-1498 are described in the prior section.

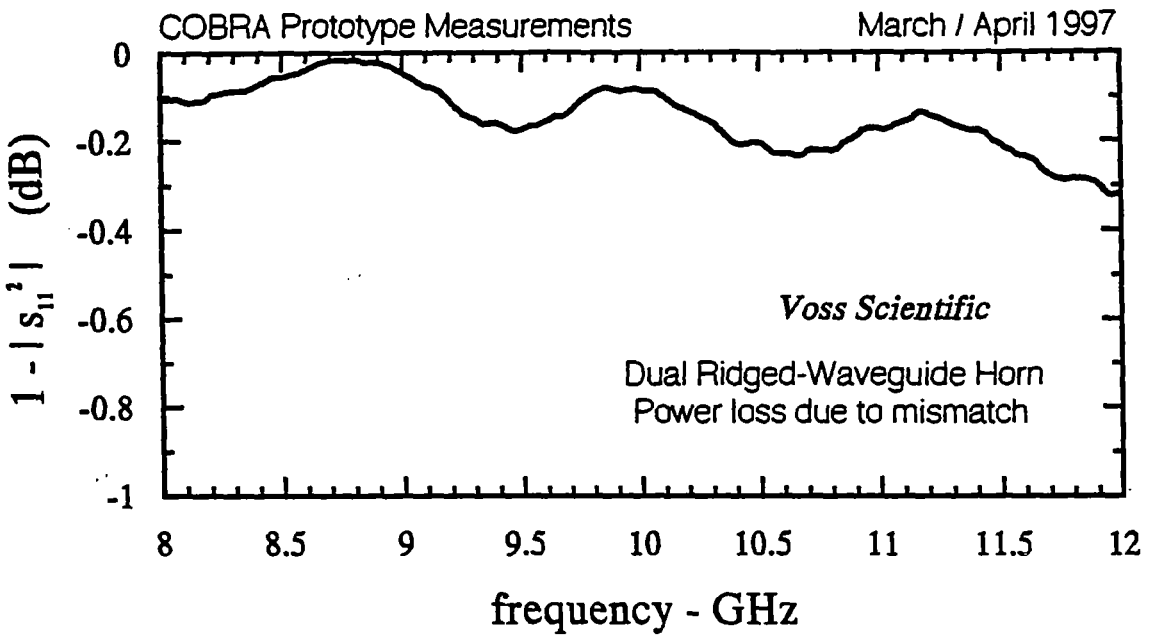

Figure 3-2 **Power loss due to impedance mismatch, as a function of frequency, of the dual-ridged waveguide horn (AEL-1498). This horn was used as one of the TX, REF and / or CAL antennas.**

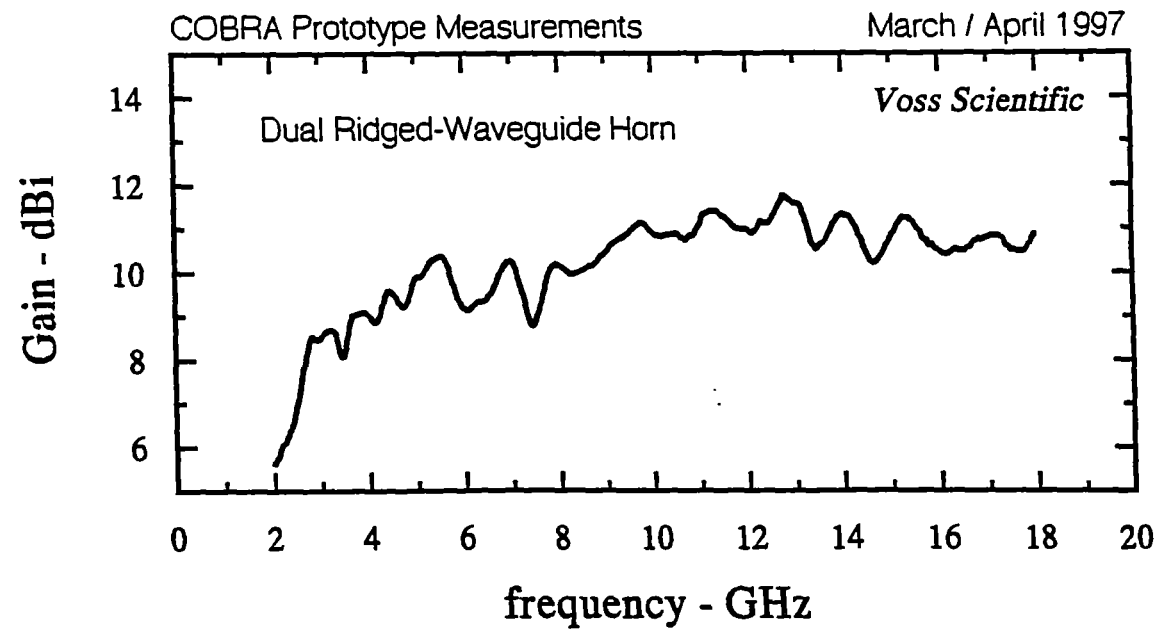

Figure 3-3 **Measured gain across the bandwidth of the AEL 1498 dual-ridged waveguide horn. This curve became part of the calibration record of the antenna measurement system.**

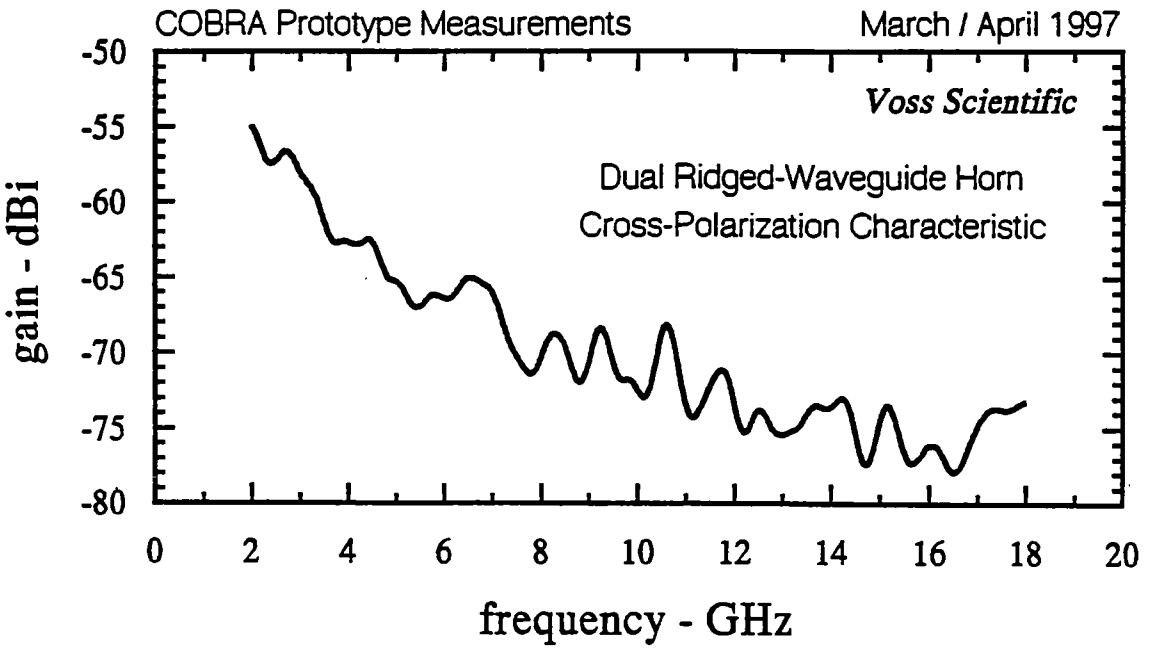

Figure 3-4 Cross-polarized gain of the AEL 1498 dual-ridged waveguide horn.

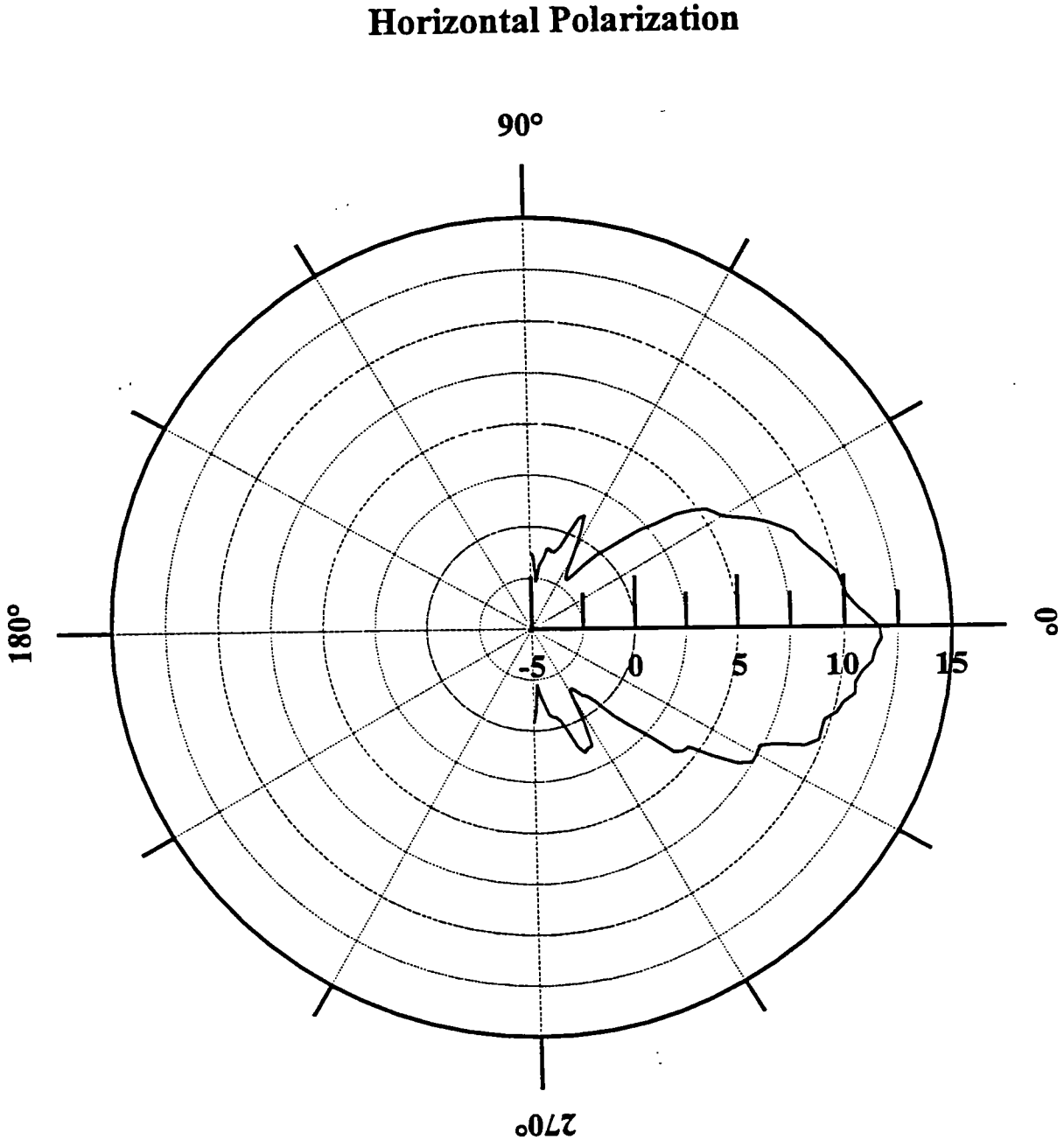

Figure 3-5 **Polar pattern of co-polarized component (horizontally polarized) of the AEL 1498 dual-ridged waveguide horn antenna radiated field. The pattern was measured at an operating frequency of 10 GHz.**

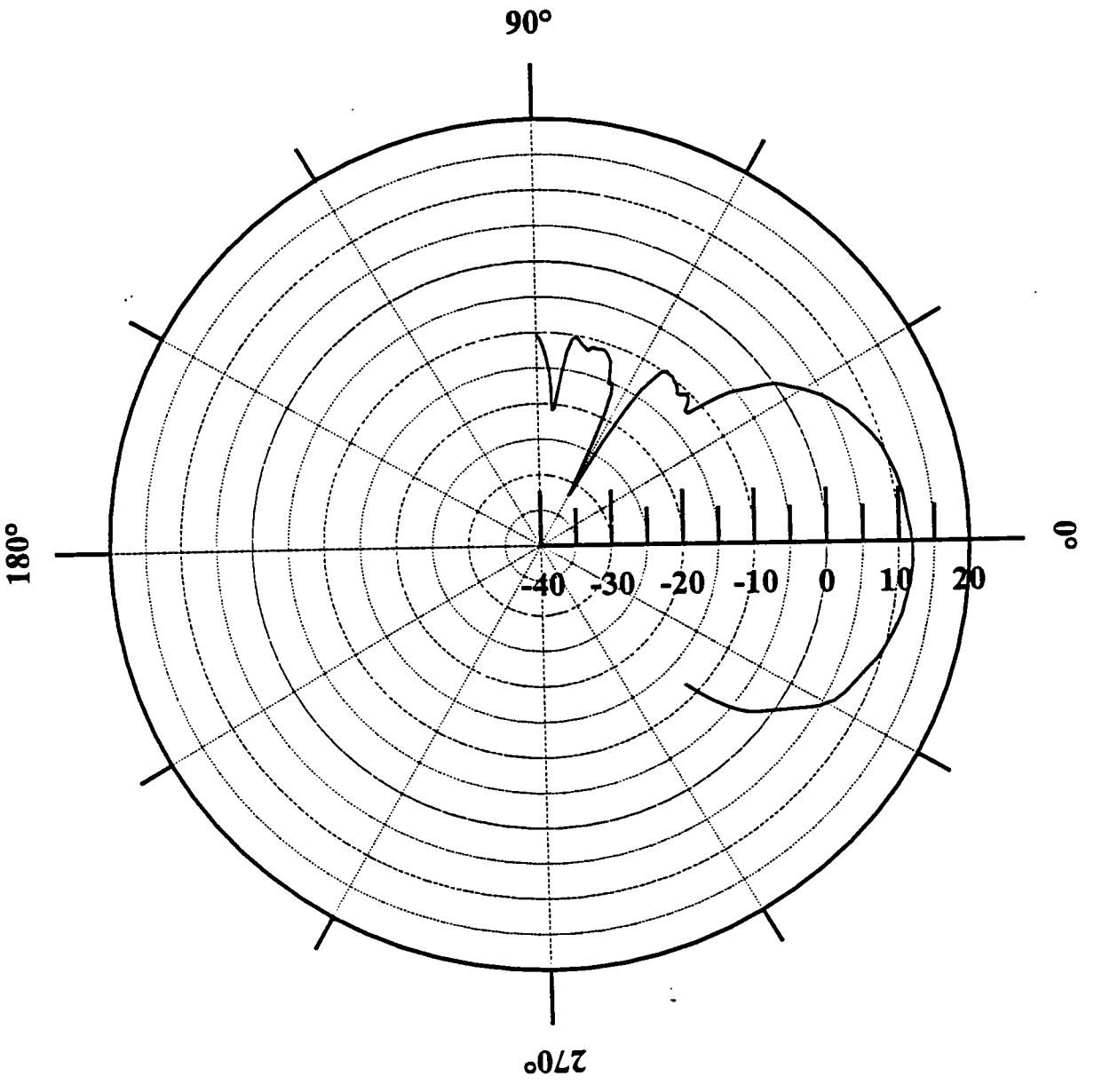

Figure 3-6 **Polar pattern of co-polarized component (vertically polarized) of the AEL 1498 dual-ridged waveguide horn antenna radiated field at 10 GHz.**

3.2.3 Calibration (CAL) Antenna

The calibration antenna used during the measurements was an X-band standard gain horn (manufacturer unknown). The antenna's input impedance was measured, and the power rejection as a function of frequency was calculated. The power rejection is shown in Figure 3-7. Note that less than 0.1 dB of power is lost to impedance mismatch over the band of interest, and the response is fairly flat.

Figure 3-8depicts the co-polarized boresight gain as a function of frequency of the X-band standard gain horn. The gain mostly rises in a linear fashion from 16 dBi at 7 GHz to 21 dBi at 14.2 GHz. Figure 3-9 depicts the cross-polarized boresight gain as a function of frequency of the X-band standard gain horn. The cross polarized gain is less than -25 dBi across the bandwidth of interest. This measurement is probably more accurate than that reported for the AEL-1498. Although its cross-polarized measured performance is not as good as commonly quoted of standard gain horns (-50 dBi), it still is acceptable for this application.

Figure 3-10 depicts the azimuthal pattern at a 10 GHz frequency for horizontal orientation (radiated electric field parallel to the chamber floor) of the X-band standard gain horn antenna. A nominal boresight gain of 18.5 dBi is indicated. Figure 3-11 depicts the azimuthal pattern for vertical orientation (radiated electric field perpendicular to the chamber floor) of the X-band standard gain horn antenna, at 10 GHz. The same boresight gain is indicated, but the sidelobes are not as large as measured when the antenna was oriented with the radiated electric field in the horizontal plane. As before, this could indicate that slightly more unwanted scattering is associated with measurements made with the horizontally polarized system antennas.

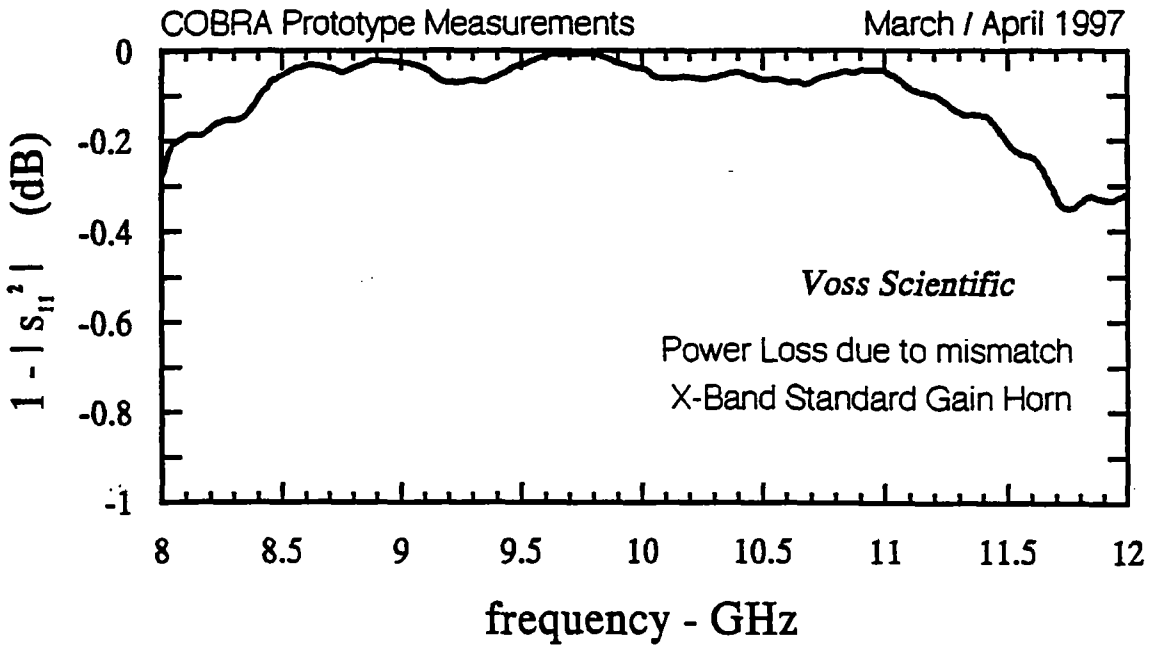

Figure 3-7 **Power loss due to impedance mismatch, as a function of frequency, of the X-band standard-gain horn antenna. This horn was used as one of the TX, REF and / or CAL antennas.**

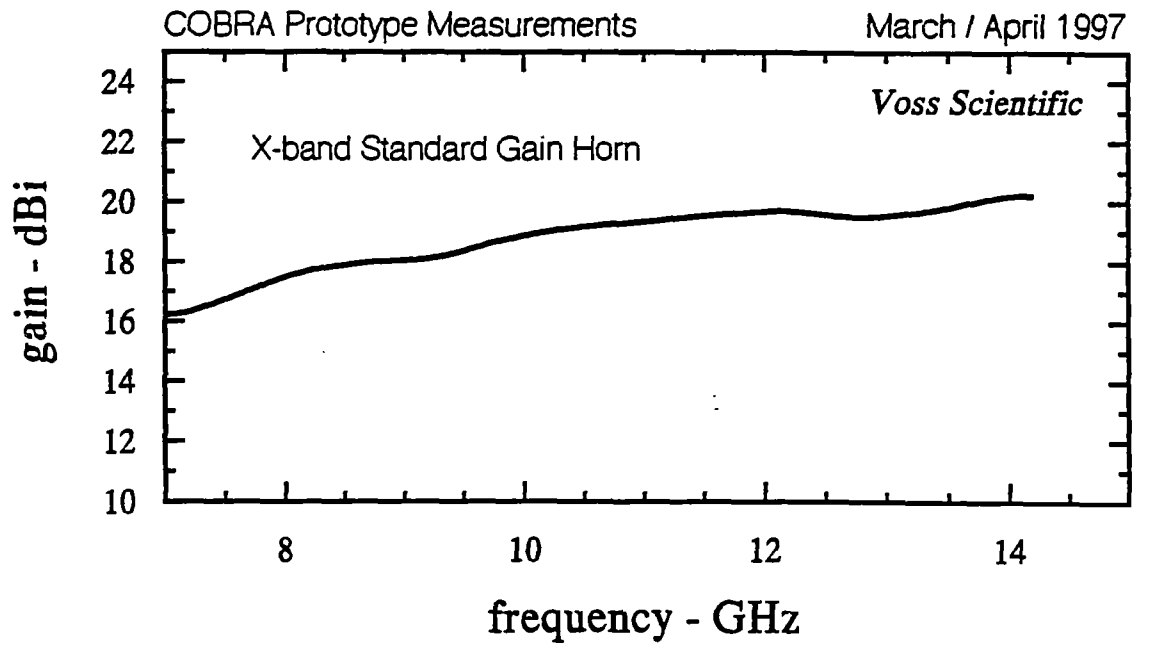

Figure 3-8 **Measured gain as a function of frequency of the X-band standard-gain horn antenna. This curve became part of the calibration record of the antenna measurement system.**

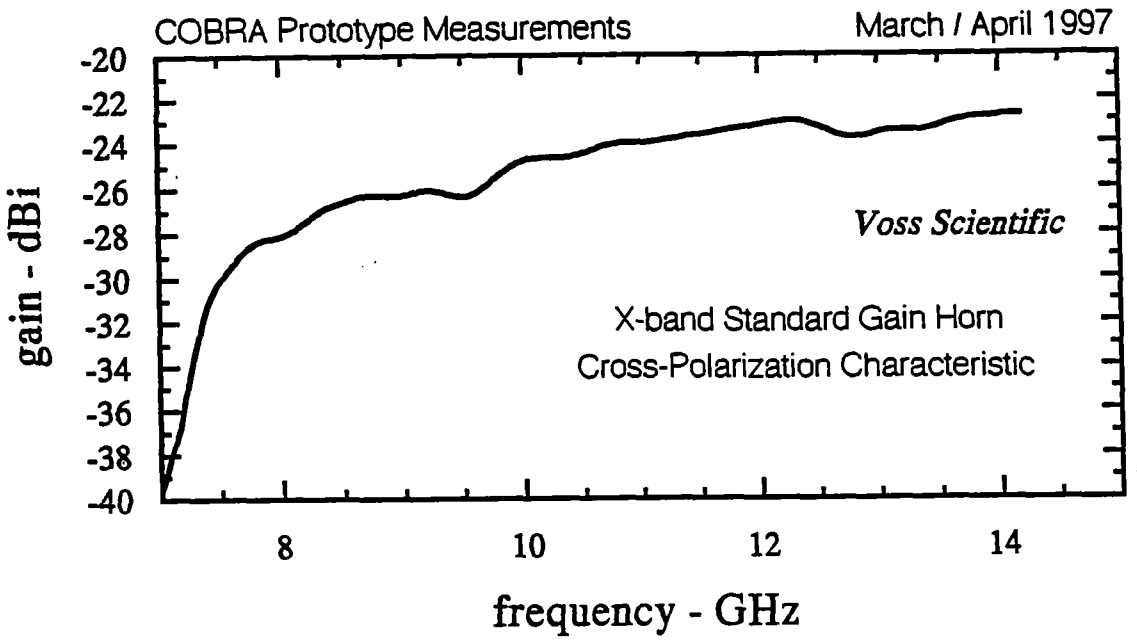

Figure 3-9 **Measured cross-polarized gain of the dual-ridged waveguide horn at 10 GHz. These values are somewhat pessimistic, the literature reports cross-polarization ratios of about 50 dB!**

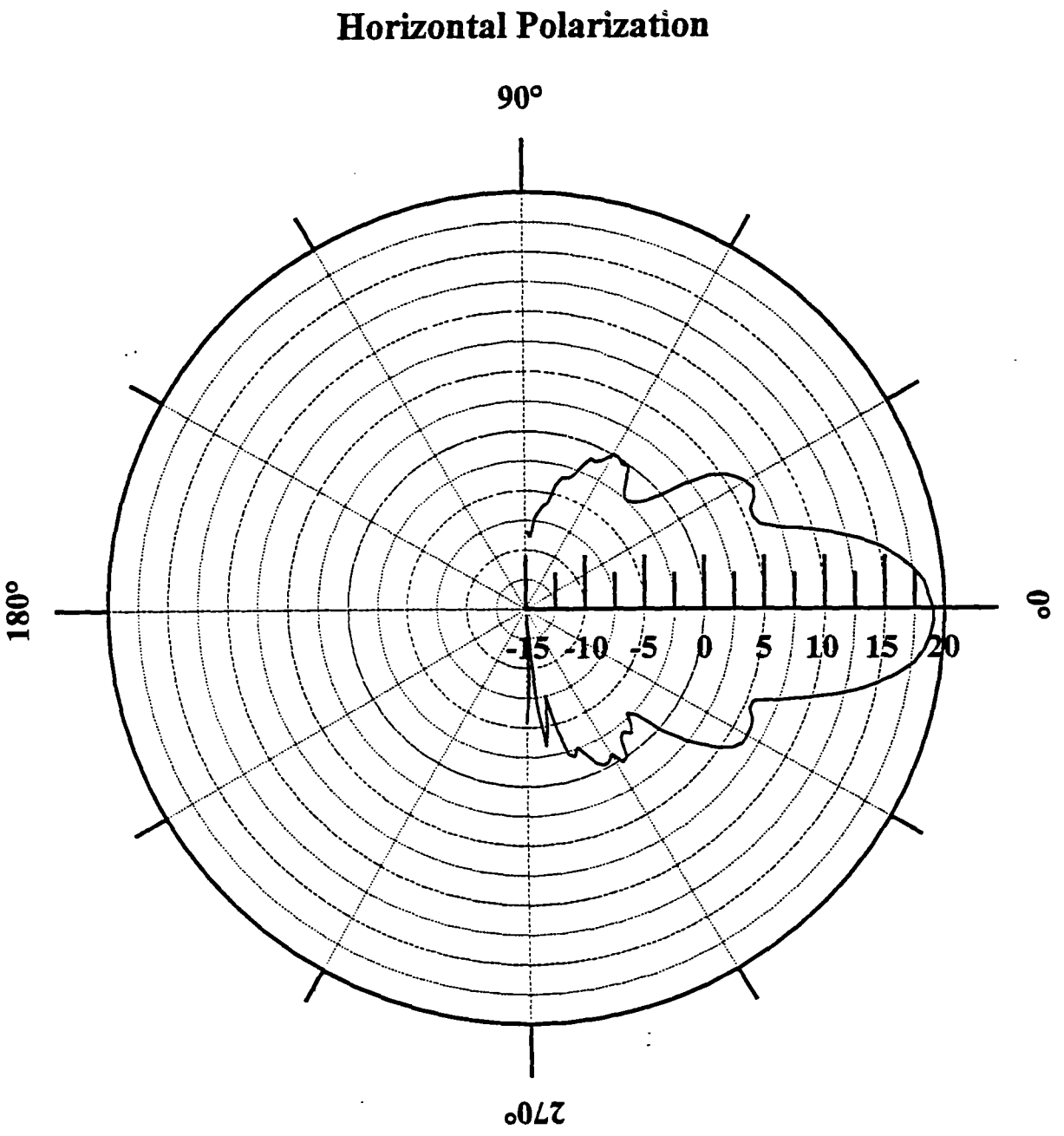

Figure 3-10 **Polar pattern of co-polarized component (horizontally polarized) of the radiated field of the X-band standard-gain horn antenna at 10 GHz.**

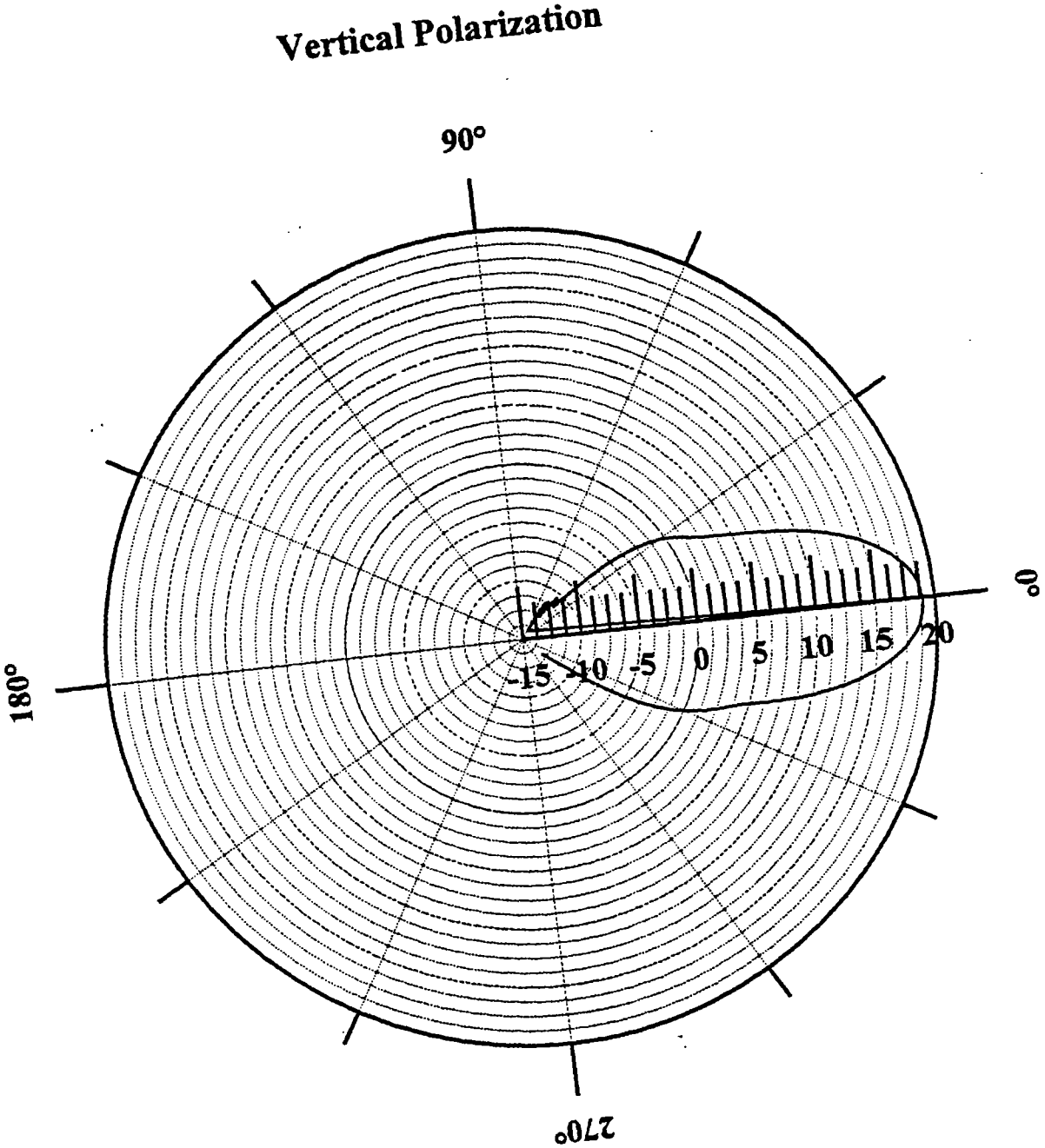

Figure 3-11 Polar pattern of co-polarized component (vertically polarized) of the radiated field of the X-band standard-gain horn antenna at 10 GHz.

4. CIRCULAR WAVEGUIDE FEED HORN CHARACTERISTICS

The mechanical characteristics of the COBRA prototype was described in detail in Section 2. There, the circular waveguide feed horn also was described. The feed horn, shown in Figure 2-1, is simply a circular waveguide (copper pipe, approx. 1.746 cm ID) driven by a custom coax-to-TM_{01} mode launcher from one end, and open at the other. This section reports the measured operating characteristics of the feed horn.

4.1 Circular Waveguide VSWR

The circular waveguide feed horn has a coaxial feed that attaches to a coax-to-TM_{01} mode launcher, a mode filter is also resident in the guide to reduce propagation of unwanted modes. Of specific interest here is the frequency dependence on the input impedance, or VSWR, of the feed horn, and the amount of power loss due to impedance mismatch. Presented earlier were the system antennas' mismatch losses as a function of frequency. These antennas were found to be well matched over the frequency band of interest, and little (< 0.2 dB) power was lost due to impedance mismatches. This is not the case for the feed horn. The input VSWR of the feed horn was measured using a standard HP8510 Vector Network Analyzer, values are shown in Figure 4-1. Figure 4-2 shows the power lost due to impedance mismatch. The impedance match is seen to be nominally acceptable at the center frequency (10 GHz), where VSWR = 2:1, and the associated mismatch power loss is -0.5587 dB. However, the match is terrible at the low end of the frequency band, where the VSWR > 10:1 at 9 GHz, and the power loss due to mismatch is -6.67 dB. The power loss due to impedance mismatch must be accounted for in the gain calculations of the COBRA prototype. Table 4-1 presents a summary of the power loss due to mismatch in the feed horn for selected frequencies across the band of interest. These values are used to compensate the measured values of gain for the mismatch loss.

For these measurements the feed horn was tuned to 10 GHz (mode launcher design, mode filter location, etc.). An objective of the Phase II program is to develop more broadband feeds. This includes development of broadband mode launchers and new feed techniques that altogether eliminate the need for a mode launcher or feed horn.

Table 4-1 A summary of the power loss values of the COBRA prototype feed horn due to mismatch as a function of frequency.

frequency (GHz)	$10\log\left\|1-\left\|s_{11}\right\|^2\right.$ (dB)
9	-6.67
9.5	-3.75
10	-0.5587
10.5	-1.141
11	-0.025

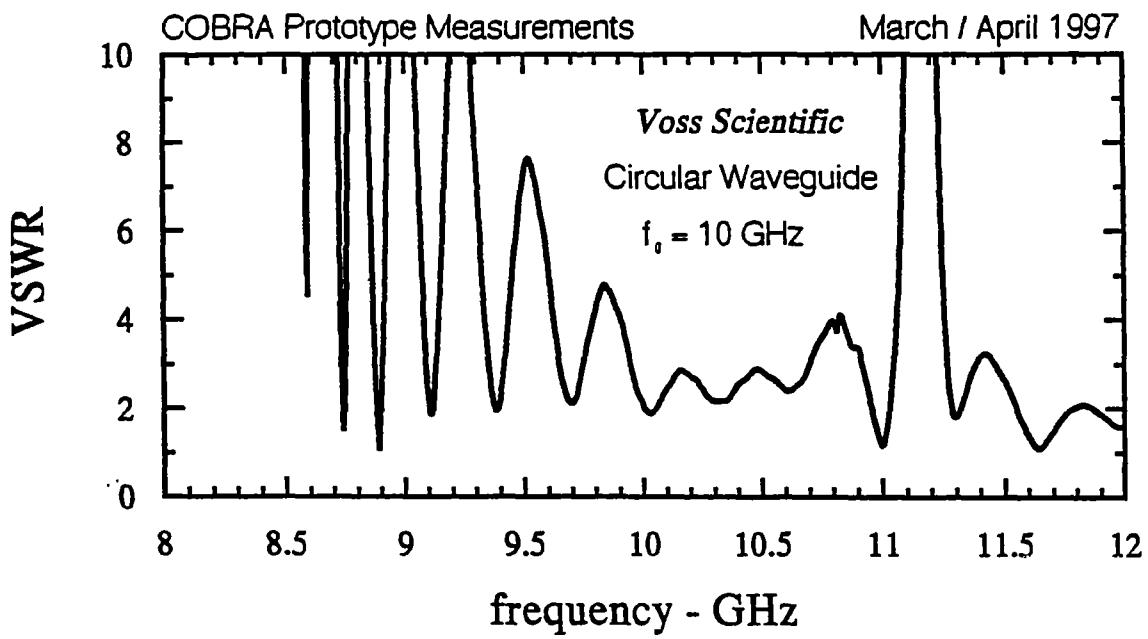

Figure 4-1 **Input VSWR, as a function of frequency, of the COBRA prototype feed horn. The feed horn was tuned nominally to 10 GHz.**

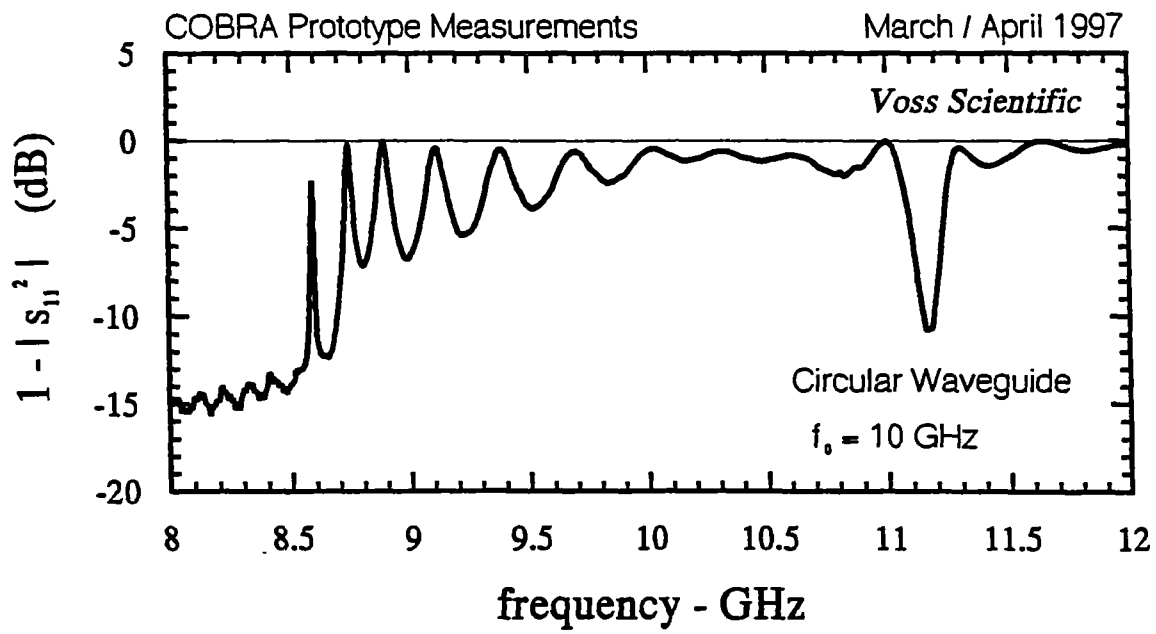

Figure 4-2 **Power loss, as a function of frequency, due to impedance mismatch of the COBRA prototype feed horn. Note the response reflects the waveguide cutoff at about 8.5 GHz.**

4.2 Circular Waveguide Feed Horn Pattern

The feed horn was detached from its mount at the focus of the COBRA prototype, and placed on a tripod, which subsequently was secured to the top of the 1-D turntable. The feed horn was connected as the AUT in the measurement system, and an azimuthal pattern was recorded.

The REF, CAL and TX horns were placed in an orientation that yielded horizontal polarization, and the azimuthal pattern was recorded. Figure 4-3 shows the measured pattern. The boresight null associated with the azimuthally symmetric pattern of the TM_{01} aperture mode is clearly indicated. The gain of the side lobes is approximately 3 dBi. The null beam width (angular separation between the -3 dB points of the peaks) is approximately 50°. The ripples in the pattern can be attributed to diffraction off of the horn rim (noticeable since the horn is small electrically and its gain is moderate) and unwanted scattering, which appears more with horizontal polarization (discussed in the prior section).

Note that although the radiated pattern of the feed horn is symmetric in terms of power density, the polarization is a function of the spatial position. For example, the pattern for the cross-polarization in the azimuthal plane is shown in Figure 4-4. For that measurement the TX, REF and CAL horns were oriented for vertical polarization. Study of the aperture distribution of the TM_{01} mode would reveal that the vertical component would ideally be zero throughout the entire azimuthal sweep. Although not "zero," it is down considerably from the co-polarized pattern, and does not exhibit the characteristic donut-hole pattern. These polarization characteristics should be reversed for the elevation pattern cut (not measured).

A scan of the feed horn pattern as a function of frequency was not performed. However, the feed horn remains electrically small over the test bandwidth, and there is no reason to believe that the feed horn pattern varied significantly over the 9-11 GHz bandwidth.

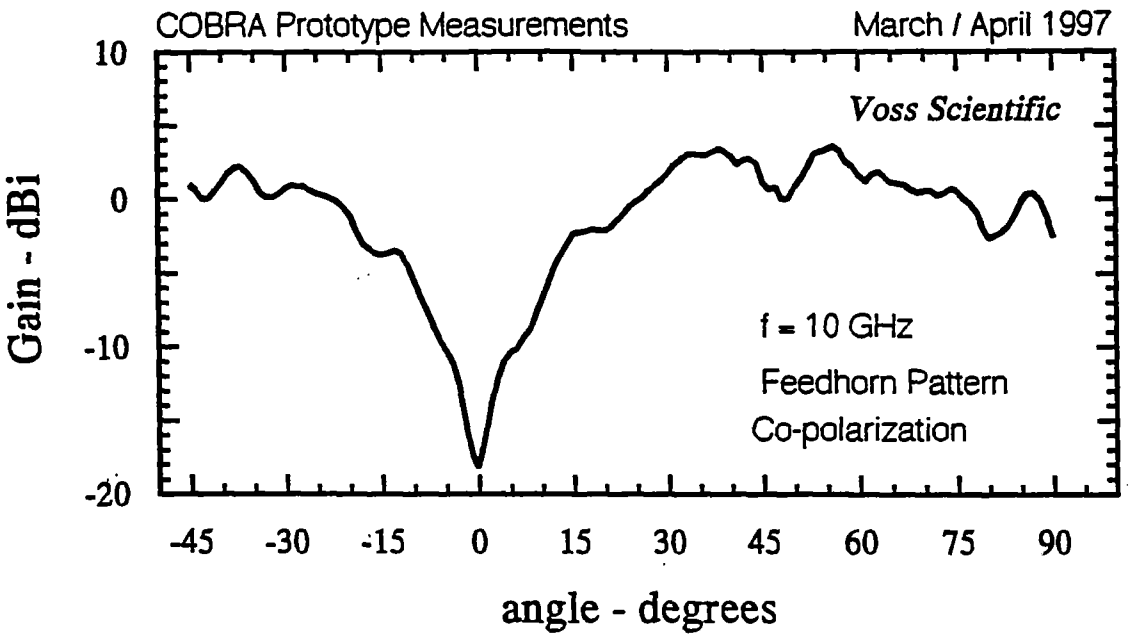

Figure 4-3 **Co-polarized pattern of the COBRA prototype feed horn in the azimuthal plane. The pattern was measured at 10 GHz.**

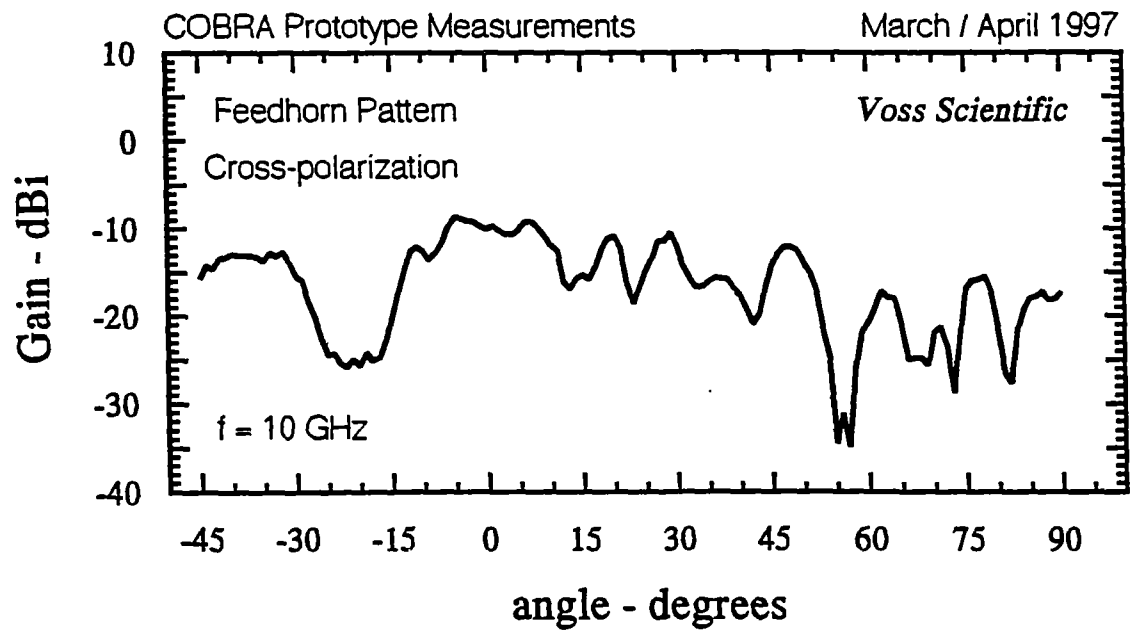

Figure 4-4 **Cross-polarized pattern of the COBRA prototype feed horn in the azimuthal plane at 10 GHz.**

5. N = 1 COBRA MEASUREMENTS

The feed horn was re-mounted at the COBRA prototype's focal point. The COBRA prototype was adjusted to an N=1 configuration (no offset given to any sector) and placed atop the wooden platform. The COBRA centerline was approximately 2.99 m (9.9125 ft.) above the chamber floor. The heights of the TX and CAL horns were made the same, and the REF antenna was placed approximately 2.134 m (7 ft.) above the floor. The lateral separation between the AUT and the REF and CAL antennas was approximately 1.83 m (6 ft.). The COBRA prototype was connected as the AUT in the system. The separation between the TX and the AUT, REF, CAL antenna suite was nominally 8.84 m (29 ft.). The next sections report on the COBRA prototype pattern dependence on the feed horn-to-COBRA vertex distance (focal length), and the polarization dependence.

5.1 Focal Point Adjustment Measurements

The COBRA prototype's F/d ratio (focal length/dish diameter) is nominally 0.375, with a 9 inch resulting focal length. The feed horn phase center then should be placed nine inches in front of the parabolic reflector's vertex. Because the phase center location of the circular waveguide feed horn was unknown, a series of measurements were made of the COBRA prototype azimuthal pattern (N=1 configuration) as the distance from the reflector's vertex to the feed horn's front plane was adjusted. These measurements were made at a 10 GHz center frequency.

Four measurements were made of the N=1 COBRA azimuthal pattern. The TX, REF and CAL horns were oriented for horizontal polarization. Measurements were made at horn-to-vertex distances of 9.5 inches, 9.75 inches, 9.825 inches, and 10 inches. Figure 5-1 shows the resulting patterns. The patterns do not differ much. They all show nominally 25 dBi of gain, and a 4° beam width (contrast this with the pattern for the feed horn); however, the pattern null does seem to skew somewhat as a function of the separation distance, and the shoulder heights are slightly un-equal for some of the measurements. The "optimum" horn to vertex distance was chosen to be 9.825-inches since this gave a null on boresight, and the most symmetric azimuthal pattern. Though the dependence was not strong, this value was retained for the remainder of the measurements.

5.2 Horizontal Polarization Azimuthal Pattern

The TX, REF and CAL horns were again oriented for horizontal polarization, and the azimuthal pattern measured for $-45^{o} \leq \varphi \leq 90^{o}$ with 1° steps. Figure 5-2 shows this pattern for a 10 GHz transmit frequency. The peak pattern gain is seen to be approximately 25 dBi, and the null beam width is about 4°. The first side lobes come in at about 7-10 dBi.

5.3 Vertical Polarization Azimuthal Pattern

A measurement of the COBRA azimuthal pattern for the TX, REF and CAL horns oriented in the vertical polarization was not made; however, we would expect the pattern to exhibit a null across the azimuthal plane based on the measurements made of the feed horn.

5.4 Frequency Dependence of the N=1 COBRA

The azimuthal pattern of the N=1 COBRA horizontal polarization was measured as a function of the frequency. Figure 5-3 shows the azimuthal patterns for $-15^{o} \leq \varphi \leq 15^{o}$, for four frequencies. One notes that all have the null on boresight, and the maximum gain increases slightly with increasing frequency (as expected since the antenna is operating quasi-optically with little or no frequency dependence).

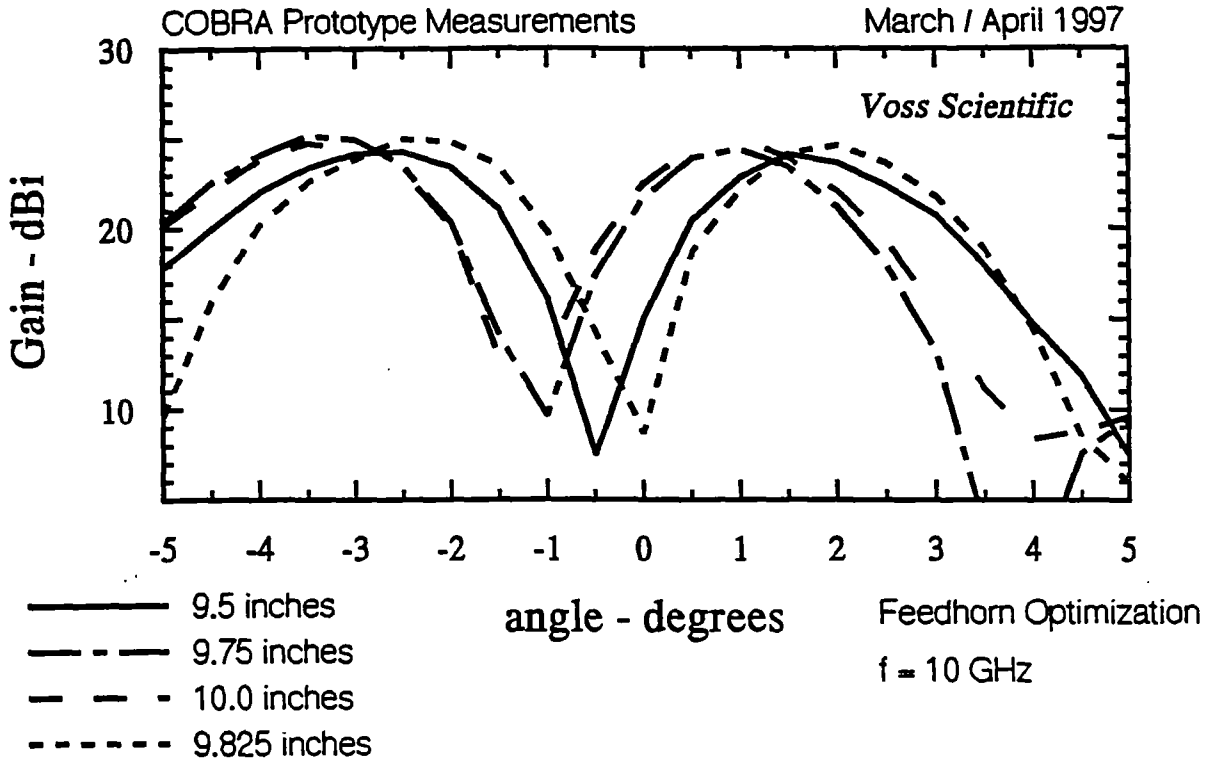

Figure 5-1 **Focal length dependence of the co-polarized pattern, in the azimuthal plane of the N=1 COBRA prototype.**

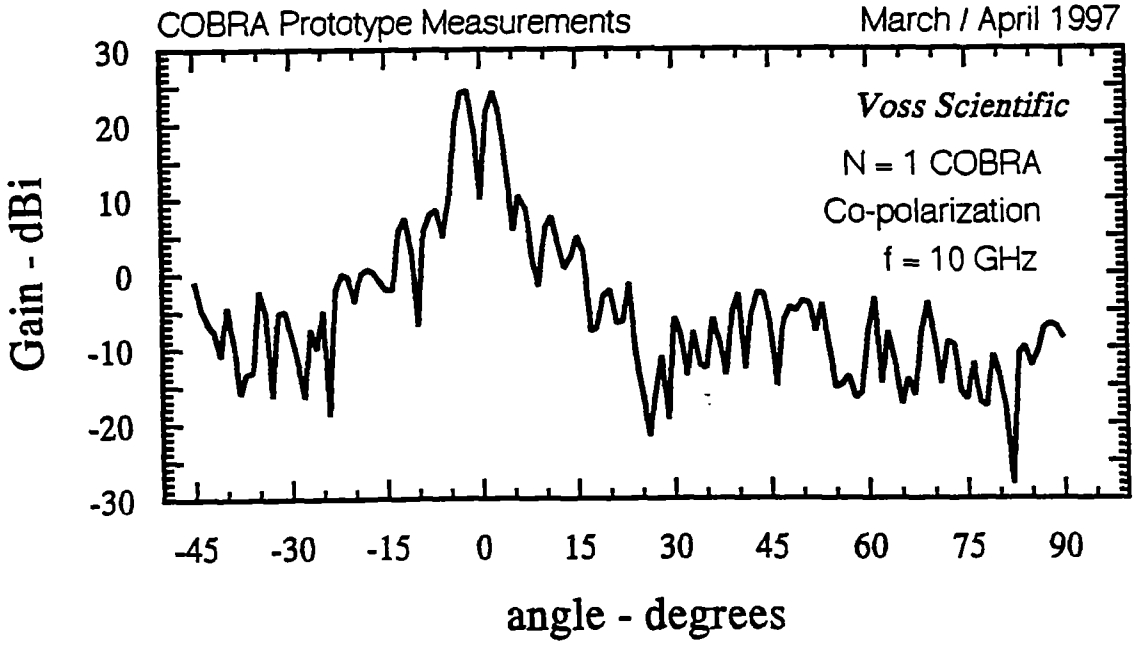

Figure 5-2 **Co-polarized azimuthal pattern of the N=1 COBRA prototype at 10 GHz.**

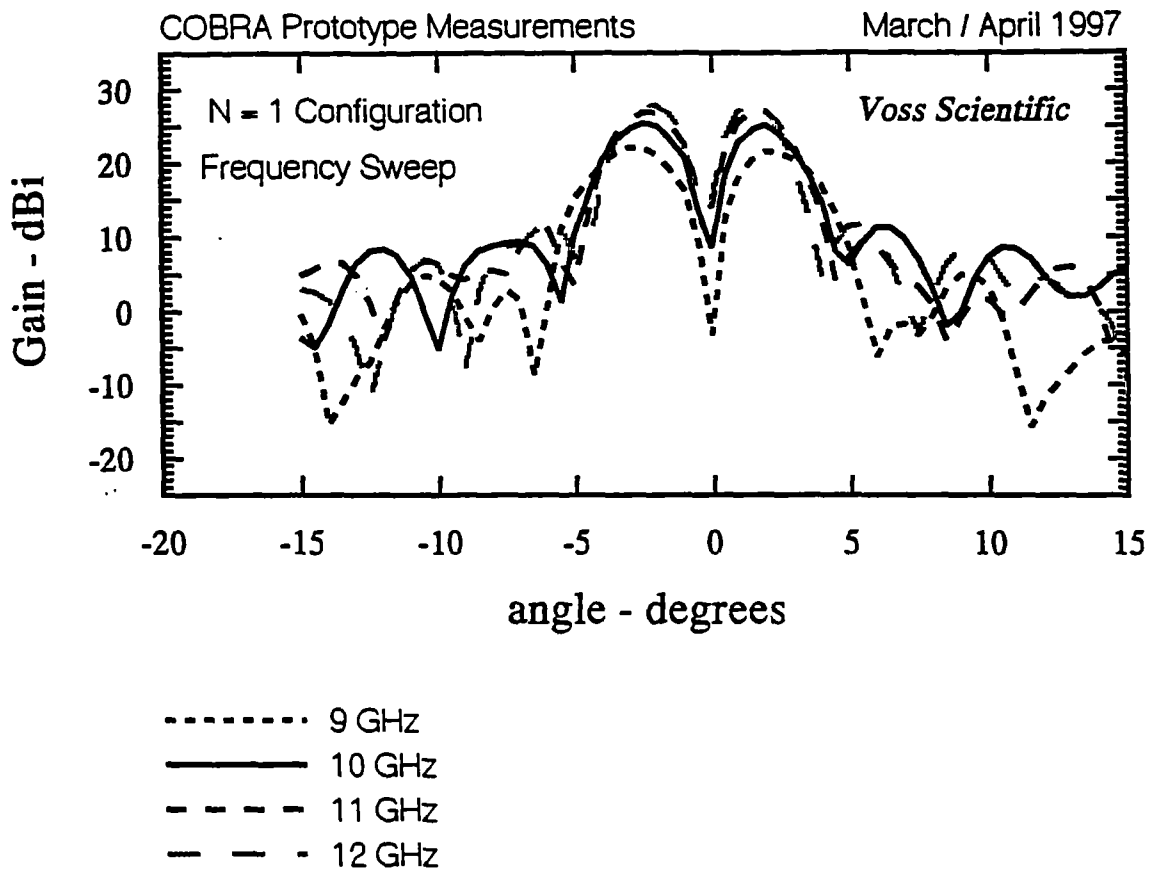

Figure 5-3 **Co-polarized azimuthal patterns for several frequencies (9, 10, 11, 12 GHz) of the N=1 COBRA prototype.**

6. N=2 COBRA MEASUREMENTS

The COBRA prototype was removed from the wooden platform, and two adjacent panels where adjusted to realize an N=2 configuration with a 10 GHz center frequency. Table 6-1 gives the relative displacement as a function of angle from the axis of the reflector (see Ref. 1).

Table 6-1 Relative sector displacements for an N=2 COBRA configuration.

θ (angle from the axis of the reflector)	τ_1 - displacement of Sector No. 1 from nominal	τ_2 - displacement of Sector No. 2 from nominal
0°	0	0.75 cm (0.295 inches)
5°	0	0.751 cm (0.2958 inches)
10°	0	0.7557 cm (0.2975 inches)
15°	0	0.763 cm (0.3004 inches)
20°	0	0.7733 cm (0.3044 inches)
25°	0	0.787 cm (0.3098 inches)
30°	0	0.804 cm (0.3165 inches)
35°	0	0.8246 cm (0.3246 inches)
40°	0	0.849 cm (0.3344 inches)
45°	0	0.879 cm (0.3459 inches)

The question "What is the focal length?" is now considered. With the COBRA main reflector sectors now offset from one another, there is no fixed vertex. The focal length (the distance from the vertex of the feed horn aperture) was fixed as follows. In this case, the mean displacement of each vertex (of each sector) was determined by

$$\bar{d} = (0 + 0.295)/2 = 0.1475.$$

The focal length then was added to this value, and the feed horn aperture was placed this distance from the vertex farthest from the feed horn. For the N=2 case, the feed horn was located $9.875 + 0.1475 = 10.0225$-inches from the vertex of Sector No. 1.

The COBRA prototype was returned to the platform and measurements of the azimuthal pattern, and the pattern frequency dependence were made. These results are reported in the following sections.

6.1 Cross-Polarization Pattern

According to the theory for a N=2 COBRA configuration, a boresight peak is achieved for one of the linear polarizations, while the second polarization continues to exhibite a boresight null. For the TX, REF and CAL horns oriented for vertical polarization, the N=2 COBRA was oriented to receive a boresight null in the azimuthal plane. Figure 6-1 shows this

pattern for a 10 GHz measurement frequency. A donut pattern with a boresight null is apparent, and the maximum gain of the pattern = 16.5 dBi.

6.2 Co-Polarized Pattern

The COBRA prototype was physically rotated 90° on the wooden platform, and the azimuthal pattern measured again. The vertical polarization orientation of the TX, REF and CAL horns was maintained. Figure 6-2 shows the resulting pattern. A boresight peak is indicated, with a 26.96 dBi maximum gain and a 3.5° beam width.

6.3 Frequency Dependence of the Co-Polarized Azimuthal Pattern

The polarization orientation of all antennas was maintained as: vertical polarization for the TX, REF and CAL horns (the co-polarized pattern of the N=2 COBRA will be vertical). Next, the azimuthal pattern was recorded for 9 GHz, 9.5 GHz, 10 GHz, 10.5 GHz, and 11 GHz. These patterns are shown in Figure 6-3, Figure 6-4, Figure 6-5, Figure 6-6, and Figure 6-7 respectively. Table 6-2 summarizes the pattern features.

The data are somewhat mixed, and a combination of factors contribute to an interpretation of the results. Over the bandwidth, the peak pattern gain varies from 24.5 dBi to 28 dBi; however, the variation is not monotonically increasing to the center frequency, then monotonically decreasing, although this would be the case were it not for the gain value measured at the center frequency. Two effects are at work. The first is the increase in the aperture size relative to wavelength, which tends to increase the gain. The second is the de-tuning effect of the parabolic reflector offset as the frequency strays from the center frequency. This tends to reduce the gain. Also, error in the value of measured gain is possible. This is particularly true of the value measured at the center frequency, a suspect number. In any event, the peak gain of the N=2 COBRA is seen not to be strongly dependent on frequency over the bandwidth of interest!

Table 6-2 Summary of the pattern characteristics, as a function of frequency, of an N=2 COBRA.

N=2 COBRA			
frequency - GHz	**Boresight Peak / Null**	**Max Gain - dBi**	**Beam Width**
9.0	peak	24.5	8.5°
9.5	peak	27.8	8.5°
10.0	peak	26.8	8.5°
10.5	peak	28	7°
11.0	peak	27	6.5°

6.4 Alternate Co-Polarized Pattern

A second primary cut is associated with the COBRA N=2 configuration. Previously, we examined the azimuthal pattern for vertical polarization of the REF, CAL and TX horns, and for both the co- and cross-polarized patterns of the COBRA. This time, the REF, CAL and TX antennas were oriented for horizontal polarization (electric field vector parallel to the floor), and the N=2 COBRA was oriented such that horizontal polarization was the co-polarized component. Figure 6-8 is the measured pattern for a 10 GHz frequency. The maximum pattern gain is 26.2 dBi, which is consistent with the data of the last section. What is somewhat surprising,, however, are the large side lobe levels. Here the side lobe levels are about 19 dBi and 21 dBi—much higher than observed in the other principal plane (6 dBi). This increase in the side lobe levels from one principal plane to the other was also observed in the N=4 measurements. The peak-to-side-lobe level is just 5 dB.

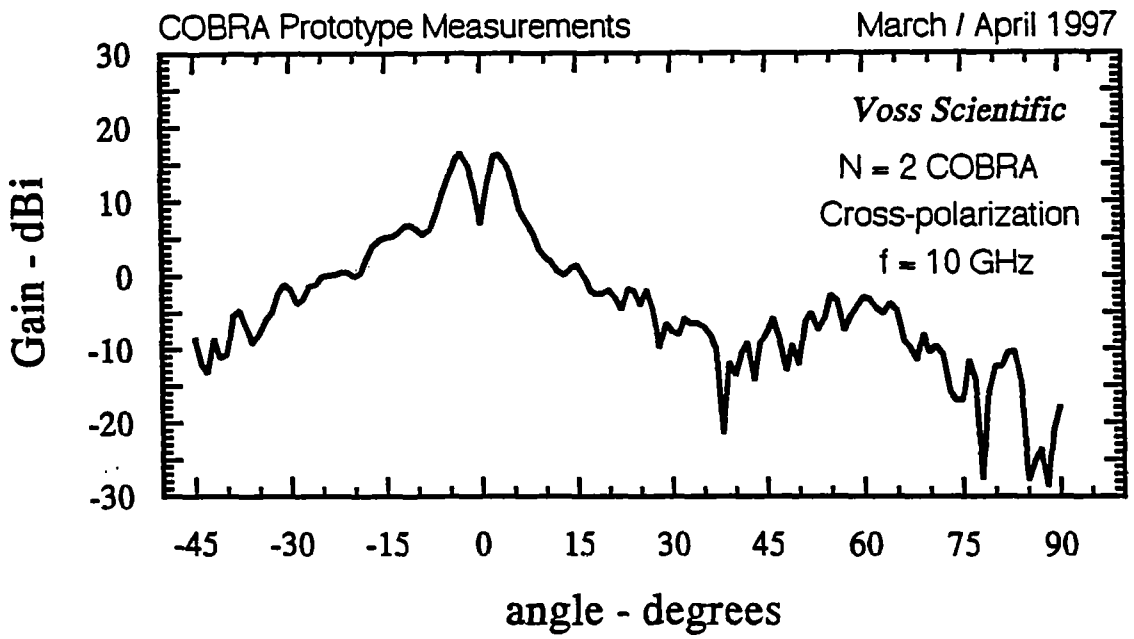

Figure 6-1 **Cross-polarized pattern of the N=2 COBRA prototype in the azimuthal plane. The measurement frequency was 10 GHz.**

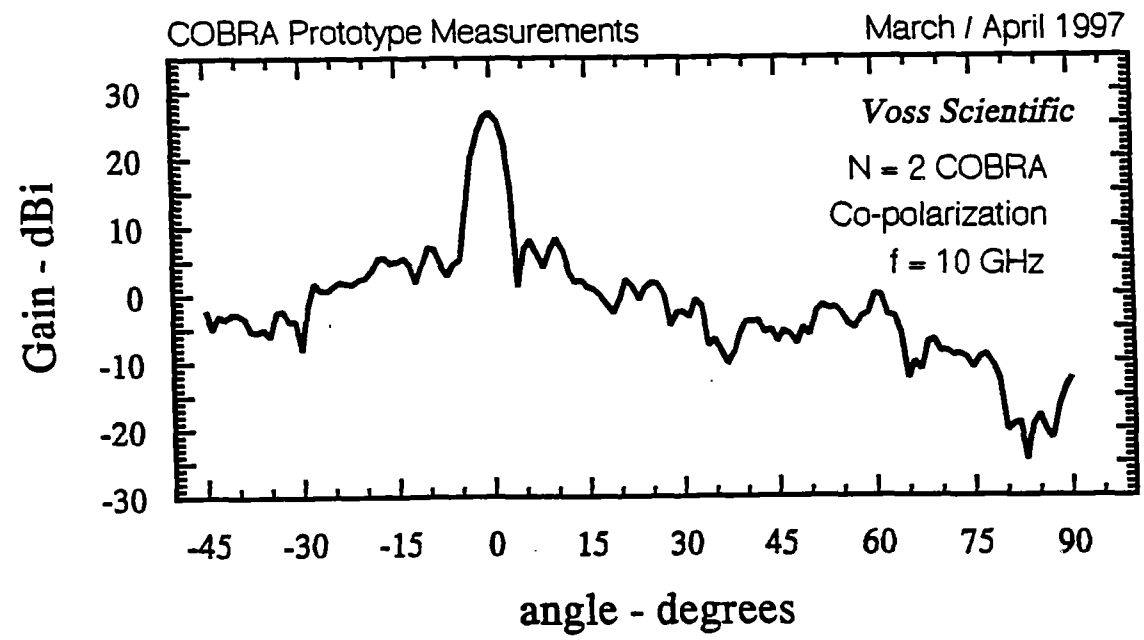

Figure 6-2 **Co-polarized pattern of the N=2 COBRA prototype in the azimuthal plane at 10 GHz.**

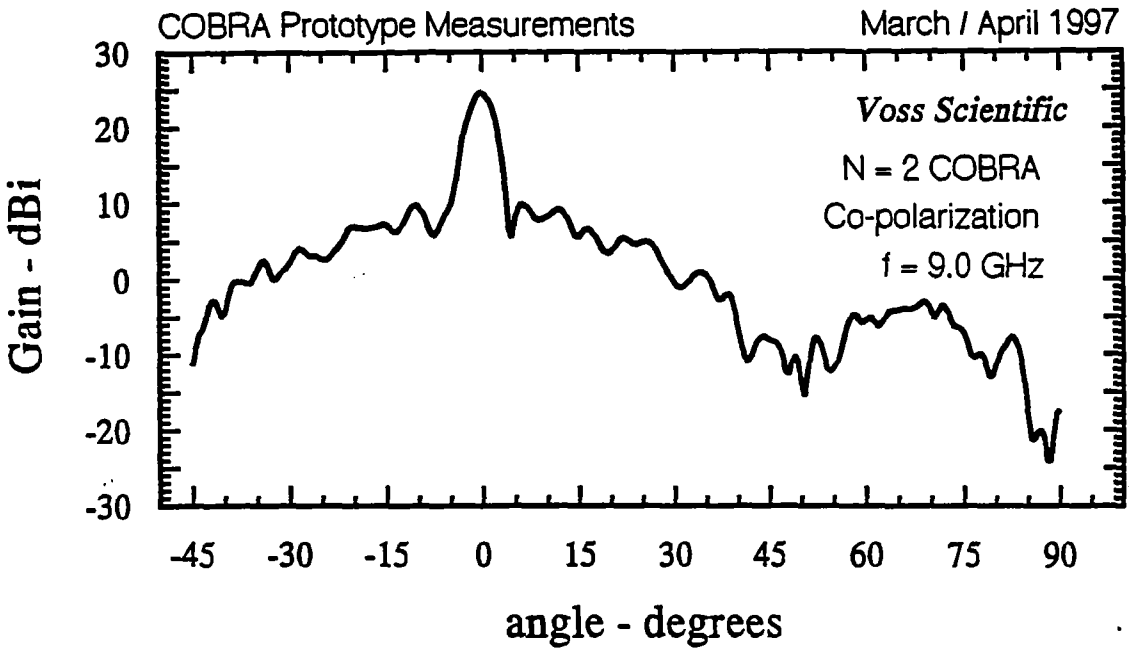

Figure 6-3 **Co-polarized pattern of the N=2 COBRA prototype in the azimuthal plane. The measurement frequency was 9 GHz.**

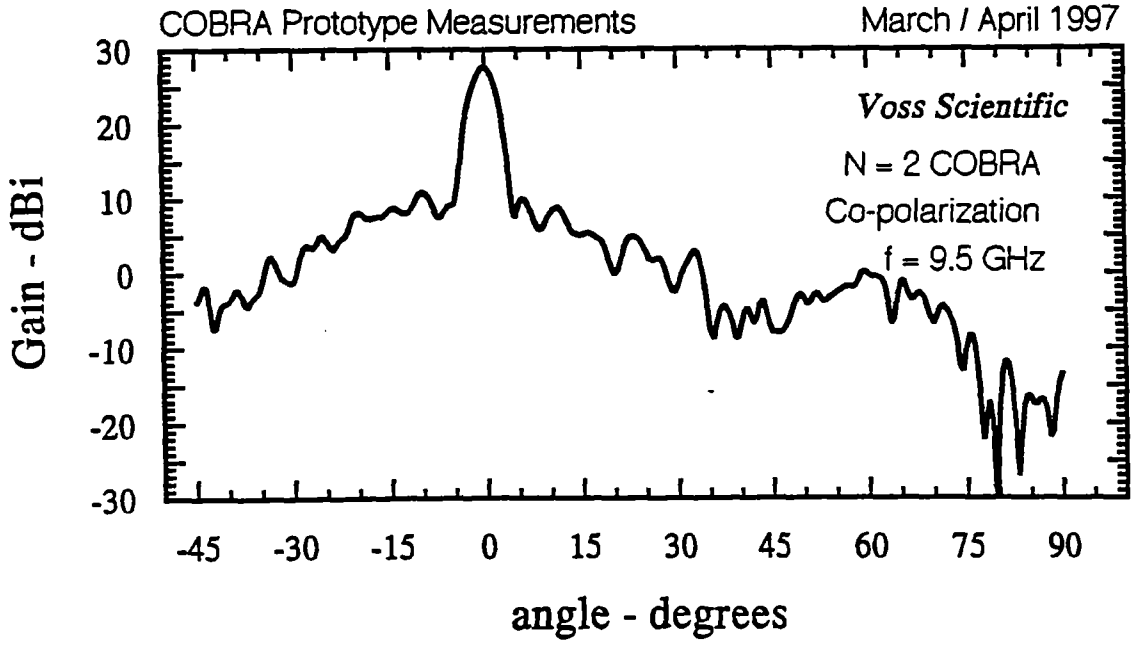

Figure 6-4 **Co-polarized pattern of the N=2 COBRA prototype in the azimuthal plane. The measurement frequency was 9.5 GHz.**

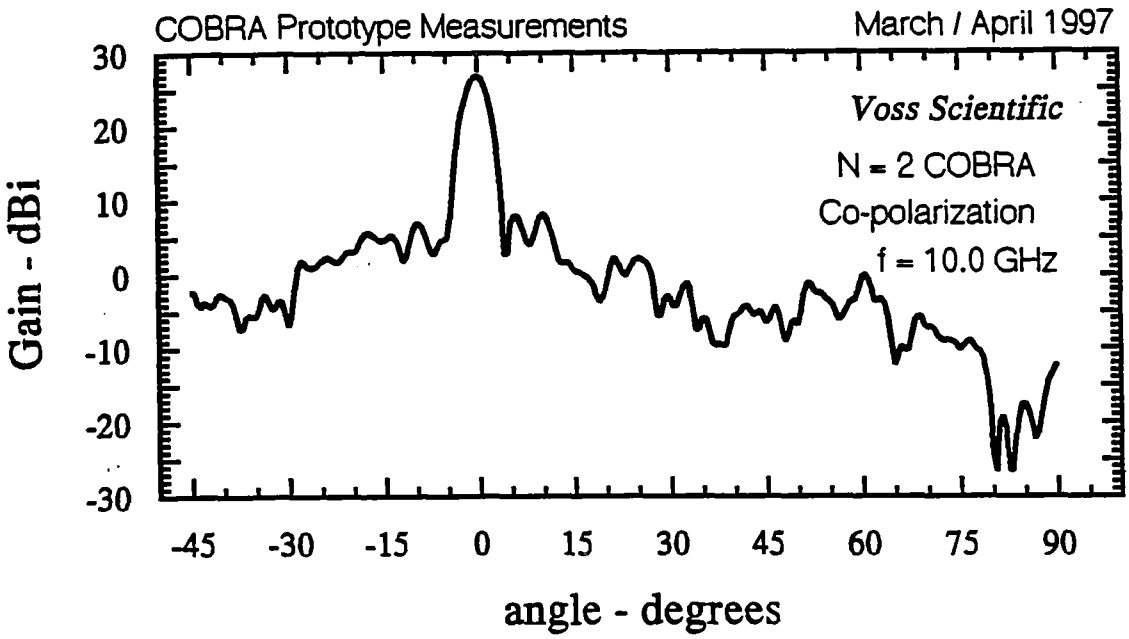

Figure 6-5 **Co-polarized pattern of the N=2 COBRA prototype in the azimuthal plane. The measurement frequency was 10 GHz. This measurement is independent of the measurement depicted in Figure 6-2.**

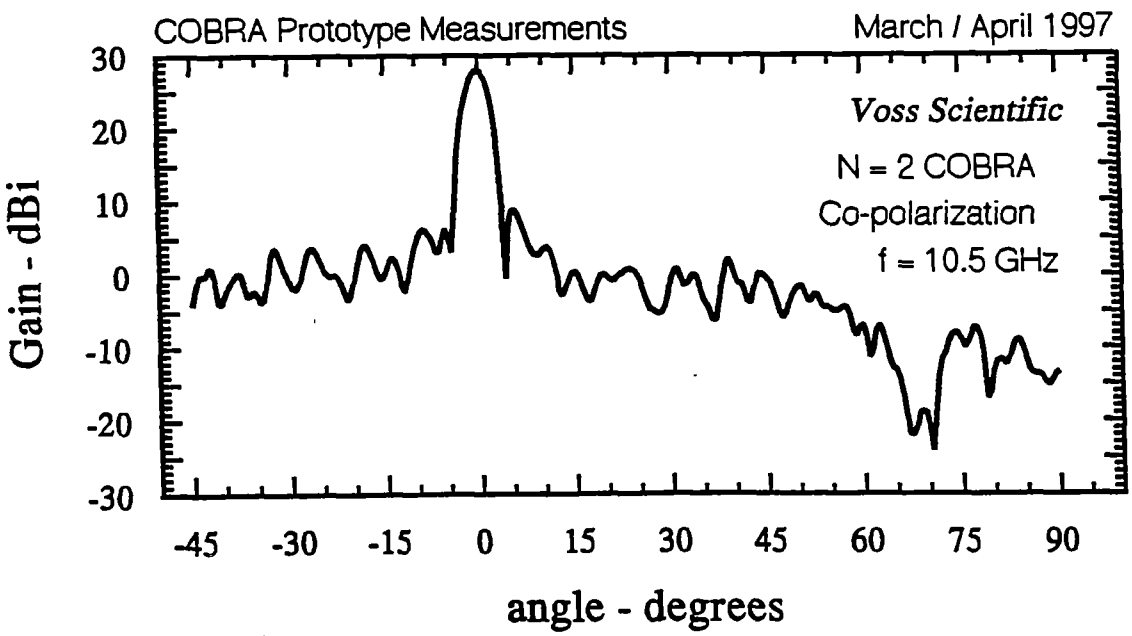

Figure 6-6 **Co-polarized pattern of the N=2 COBRA prototype in the azimuthal plane. The measurement frequency was 10.5 GHz.**

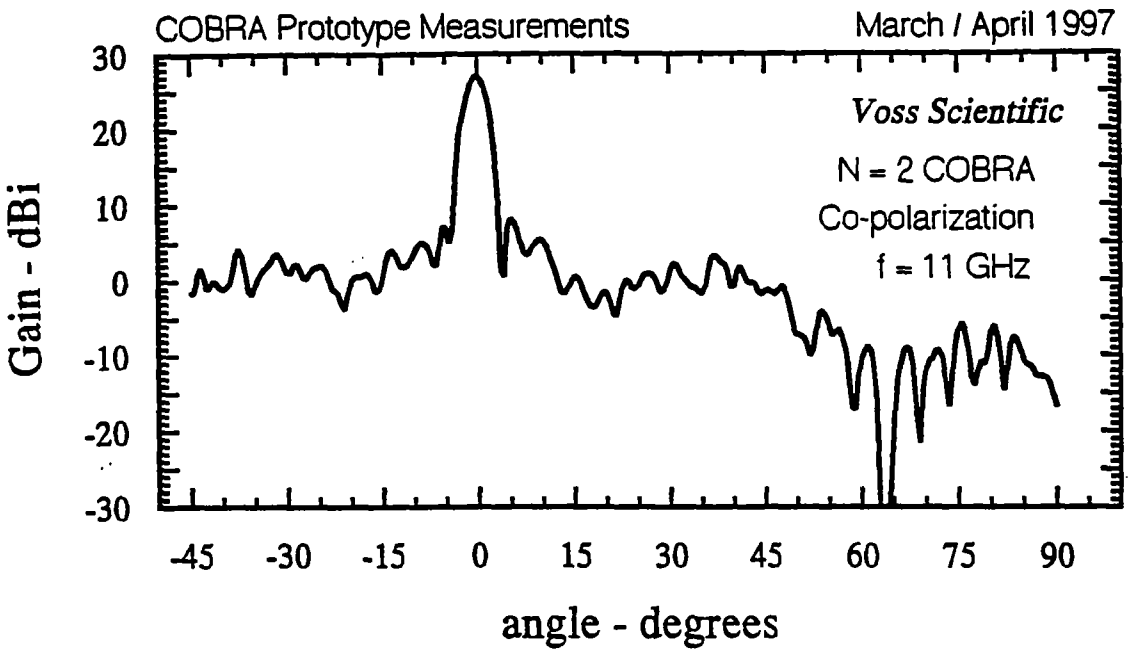

Figure 6-7 **Co-polarized pattern of the N=2 COBRA prototype in the azimuthal plane. The measurement frequency was 11 GHz.**

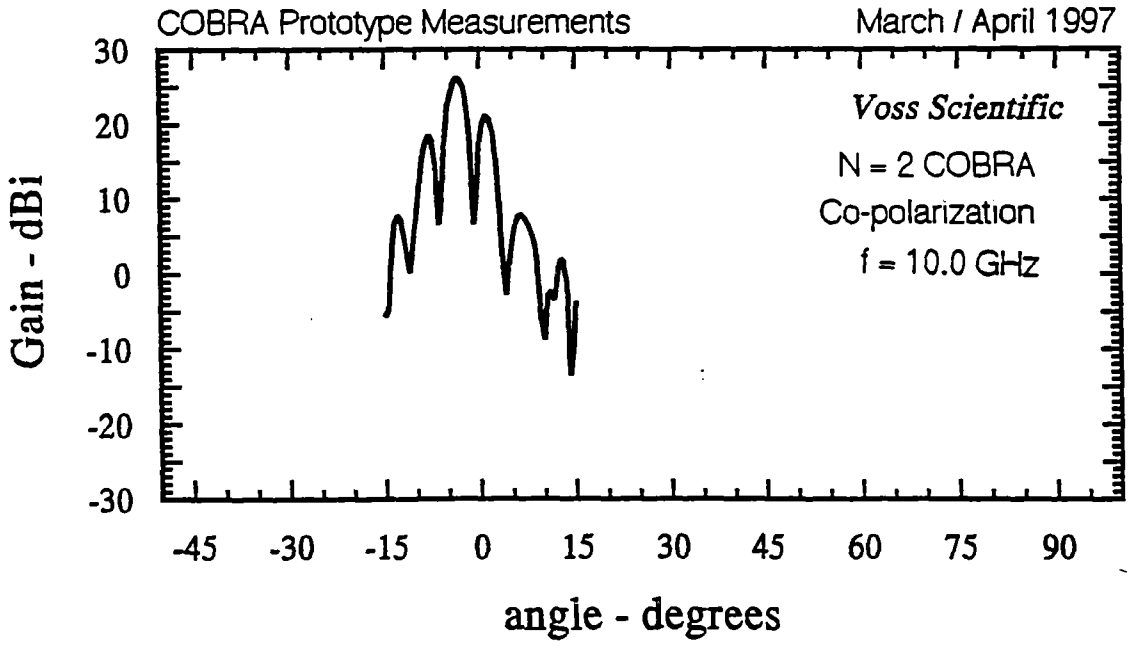

Figure 6-8 **Co-polarized pattern of the N=2 COBRA prototype in the elevation plane. The measurement frequency was 10 GHz.**

7. N=4 COBRA MEASUREMENTS

The COBRA prototype again was removed from the wooden platform, and the four sectors were adjusted to realize an N=4 configuration with a 10 GHz center frequency. Table 7-1 gives the relative displacement, as a function of angle from the reflector axis (see Ref. 1).

The focal length (distance from the feed horn aperture to the paraboloid vertex) was fixed as follows. The mean displacement of each vertex (of each sector) was determined as before, in this case

$$\bar{d} = (0 + 0.1475 + 0.295 + 0.4426)/4 = 0.22127 .$$

The nominal focal length then was added to this value, and the feed horn aperture was placed this distance from the vertex of the paraboloid sector that remained fixed (at its nominal N = 1 position). For N=4, the feed horn was located $9.875 + 0.22127 = 10.0963$ inches from the vertex of Sector No. 1.

The COBRA prototype was returned to the platform, and measurements of the azimuthal pattern and pattern frequency dependence were made. These results are reported in the following sections.

7.1 N=4 : Tx Horn = Horizontal Polarization

The theory of the COBRA operation predicts that circular polarization is achieved for N=3 and all higher N-values. The REF, TX and CAL antennas were oriented for horizontal polarization. Figure 7-1 shows the measured azimuthal pattern at the 10 GHz center frequency. This pattern has several interesting aspects. Its peak (23.5 dBi) is achieved on boresight, but this is down from the N=2 pattern peak (26.8). Both are predicted in the theory, but note that we again see large side lobe levels for this polarization. The peak-to-side lobe ratio is 5 dB—the same as the N=2 case.

Table 7-1 Relative sector displacements for an N=4 COBRA configuration.

θ (angle from the axis of the reflector)	τ_1 – nominal configuration	τ_2 - displacement of Sector No. 2 from nominal cm (inches)	τ_3 - displacement of Sector No. 2 from nominal cm (inches)	τ_4 - displacement of Sector No. 2 from nominal cm (inches)
0°	0	0.374 (0.1475)	0.749 (0.295)	1.124 (0.4426)
5°	0	0.375 (0.1478)	0.751 (0.2956)	1.126 (0.4435)
10°	0	0.378 (0.1487)	0.755 (0.2973)	1.133 (0.4460)
15°	0	0.381 (0.1501)	0.763 (0.3002)	1.143 (0.4502)
20°	0	0.386 (0.1521)	0.773 (0.3042)	1.159 (0.4564)
25°	0	0.393 (0.1548)	0.786 (0.3096)	1.179 (0.4644)
30°	0	0.402 (0.1581)	0.803 (0.3163)	1.205 (0.4744)

35°	0	0.412 (0.1622)	0.824 (0.3244)	1.236 (0.4866)
40°	0	0.424 (0.1671)	0.849 (0.3342)	1.273 (0.5012)
45°	0	0.439 (0.1728)	0.878 (0.3457)	1.317 (0.5185)

7.2 N=4 : TX Horn = Vertical Polarization

Next, the REF, TX and CAL antennas were oriented for vertical polarization. Figure 7-2shows the measured azimuthal pattern, at the 10 GHz center frequency. Again, a boresight peak is observed, with a 23.1 dBi maximum gain. Notice how low the side lobe levels are for this polarization. The peak-to-side lobe ratio is almost 20 dB!

7.3 Frequency Dependence of the Azimuthal Pattern

The polarization of the TX, REF and CAL horn antennas was maintained as vertical, which should give a large pattern peak-to-side lobe ratio (as seen above). The azimuthal pattern was recorded for 9 GHz, 9.5 GHz, 10 GHz, 10.5 GHz, and 11 GHz. These patterns are shown in Figure 7-3, Figure 7-4, Figure 7-5, Figure 7-6, and Figure 7-7 respectively. Table 7-2 summarizes the pattern features.

The data again are somewhat mixed, as was the N=2 data. Over the bandwidth, the peak pattern gain varies from 20.87 dBi to 23.8 dBi. The first observation is that the gain value is down from the N=2 configuration. In fact, the values are down approximately 3-5 dB over the measured bandwidth. The theory developed in Reference 1 predicts that the gain for each linear component of the N=4 configuration will be down 3 dB from the gain of the single linear component of the N=2 configuration. The 3 dB beam widths for the N=4 patterns are narrower than their N=2 counterparts, a paradox in a sense since lower gain normally implies broader beam width. In any event, the peak gain and patterns of the N=4 COBRA are again seen to be not strongly dependent on the frequency over the bandwidth of interest!

7.4 Boresight Phase Relations

Measurements of the azimuthal patterns of both N=4 configuration polarizations (including the boresight gain) have shown that their peak boresight gains are 23.1-dBi and 23.5-dBi. This is consistent with the predicted circularly polarized nature of the boresight field of the N=4 configuration; however, it is not a sufficient condition. Depending on the reference, the phase relationship between the two polarizations should be ±90°. One polarization should lead or lag

Table 7-2 Summary of pattern characteristics, as a function of frequency, of an N=4 COBRA.

N=4 COBRA			
frequency - GHz	**Boresight Peak / Null**	**Max Pattern Gain**	**Beam width**
9.0	Peak	20.87	4.5°

9.5	Peak	23.5	4.5°
10.0	Peak	22.7	3.5°
10.5	Peak	23.8	3.5°
11.0	Peak	22.1	5.5°

the other polarization by 90°. These measurements were to measure the magnitude and phase relationship of the boresight field of the N=4 COBRA. The measurement technique is described first, then the measurement results are presented.

7.4.1 Circular Polarization Measurement Procedure

The standard Narrowband Antenna Measurement System configuration is not convenient for vector, phase-referenced measurements of two independent quantities (the two linear polarizations of the assumed circularly polarized N=4 COBRA boresight field). But with a manual operating procedure and slight modifications in the manner in which the antennas (AUT, REF, TX and CAL) are connected to the system, a phase-referenced measurement of the boresight characteristics is possible.

To begin, the REF and TX antennas were mounted on a circular piece of fiberglass. The CAL antenna was not used during this measurement, since we were looking to measure just the relative differences between the boresight magnitude and phase of each linear polarization. The fiberglass was drilled in four places along its perimeter at equiangular intervals. A fiberglass post (2 inches wide, $^1/_8$ inch thick, 12 inches long) was fabricated with two mounting holes, and a tripod mounting grip assembly on one end. The antennas were attached to the fiberglass post with two nylon screws, and mounted to the tripods through the tripod mounting grip. This permitted the antennas to be rotated 90° in a very accurate manner, without adjusting the tripod heads or moving the tripods (thus maintaining the TX / RX horn separation). This was important given the wavelength of the center frequency (λ = 29.998 mm at 10 GHz), and the objective of measuring relative phase to single digit degree accuracy (0.08328 mm/deg.).

Next, the HP8510 controller was placed in manual mode (from the front panel), and set to sweep across the 9 - 11 GHz bandwidth. The transmit power was set to 10 dBm, and 801 points across the band was specified. The REF channel was connected to the B1 channel of the custom S-parameter test set, and the AUT was connected to channel B2 (see Figure 3-1). A sweep was conducted, and the data downloaded onto a floppy disk.

Next, the TX and REF antennas were removed from their tripods. The fiberglass post was removed from the circular pad, rotated 90° and re-attached. The antennas were returned to the tripods. A second sweep and measurement was conducted, and the display data again were downloaded onto a floppy disk.

The key to this measurement technique is to make the measurements within the smallest possible time interval. The measurement depends on the Antenna Measurement System's frequency sources not drifting in phase over the time interval associated with the two

measurements. For this reason, the measurements are made as quickly as possible, and the frequency sources on the transmit and receive sides are not turned off between measurements.

7.4.2 Circular Polarization Measurement Results

The data taken from the HP8510 controller were processed to yield relative magnitude and relative phase (absolute phase difference) for each measurement. Figure 7-8shows the magnitude (relative) variation as a function of frequency of the horizontal polarization. The magnitude (relative) variation, as a function of frequency, of the vertical polarization is shown in Figure 7-9. One notes a definite frequency dependence on the received signal, and a great deal of variation is due to the frequency dependence of the COBRA feed horn's input impedance. However, the objective here is to measure the relative differences between the two polarizations, and compensation is not required since the same effect is present in both measurements. Figure 7-10 shows the phase (relative) variation as a function of frequency of the horizontal polarization. Figure 7-11 shows the phase (relative) variation as a function of frequency of the vertical polarization. One notes that the phase wraps between $-90^{o} \leq \varphi \leq 90^{o}$ for the measured phase of the two polarizations (an artifact of the HP8510). The absolute phase difference between the two polarizations is simply the difference between the two relative measurements at a particular frequency.

Table 7-3 summarizes the measurement data. There, the differences in the phase and magnitudes of the two linear polarizations are indicated. One notes that the field is remarkably broadband across the entire measurement bandwidth. The phase deviates from the ideal by only 13° at a maximum over the bandwidth. The magnitude deviation becomes 3 dB at higher frequencies, and is a minimum at the bandwidth's low end.

Table 7-3 Summary of the boresight polarization characteristics, as a function of frequency, of an N=4 COBRA.

N=4 COBRA Boresight Polarization Properties		
Frequency - GHz	$\Delta\varphi$	Δ-magnitude (dB)
9.0	83.8°	-0.21
9.5	97.96°	-0.61
10.0	95.17°	-1.67
10.5	77.85°	-3.00
11.0	103.07°	-2.59

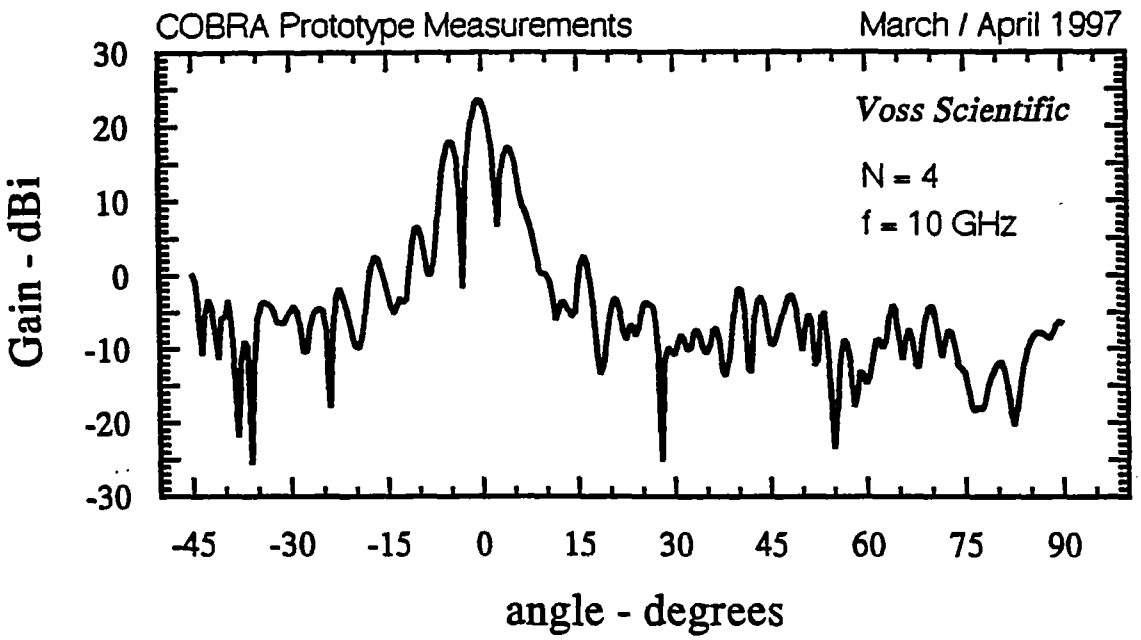

Figure 7-1 **Co-polarized pattern of the N=4 COBRA prototype in the elevation plane. The measurement frequency was 10 GHz.**

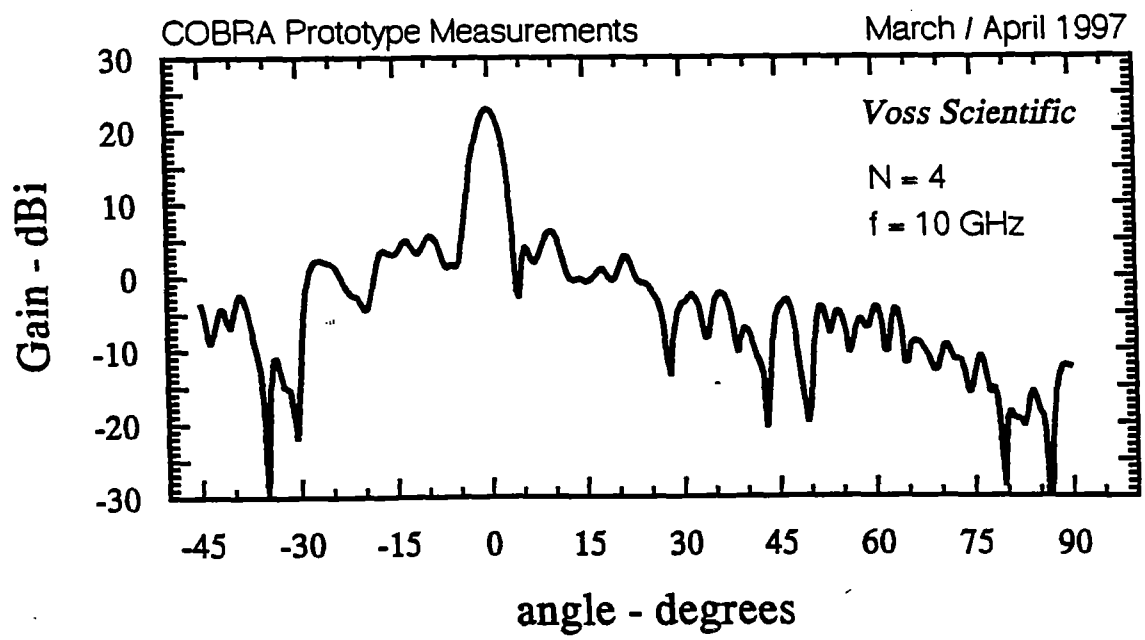

Figure 7-2 **Co-polarized pattern of the N=4 COBRA prototype in the azimuthal plane. The measurement frequency was 10 GHz.**

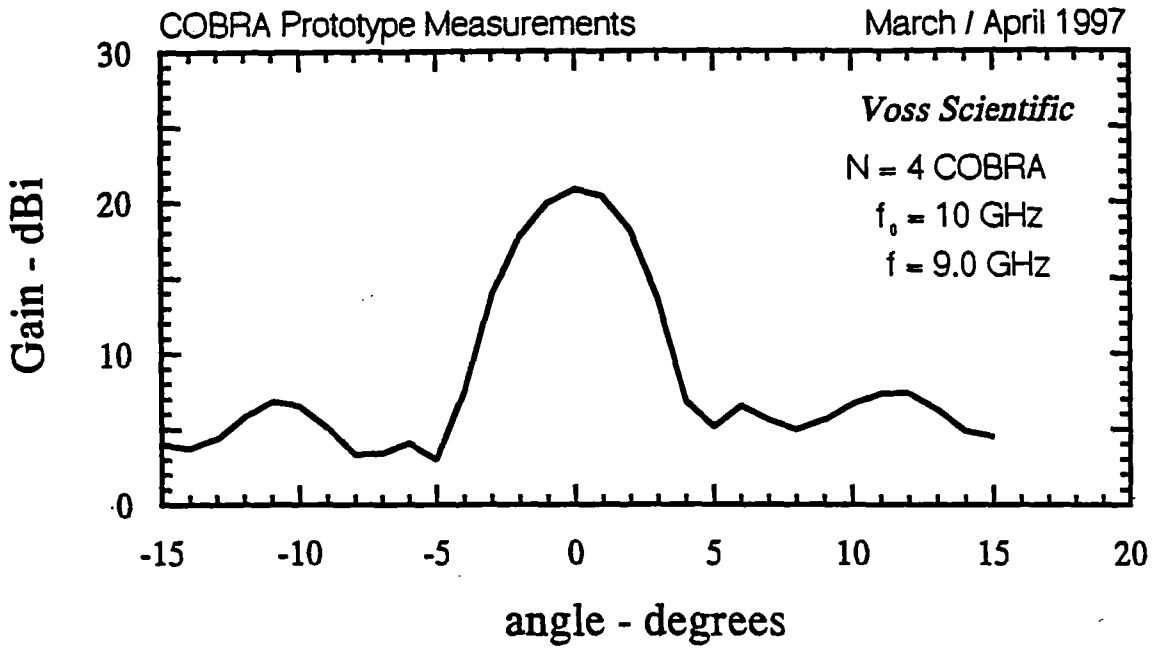

Figure 7-3 **Co-polarized pattern of the N=4 COBRA prototype in the azimuthal plane. The measurement frequency was 9 GHz.**

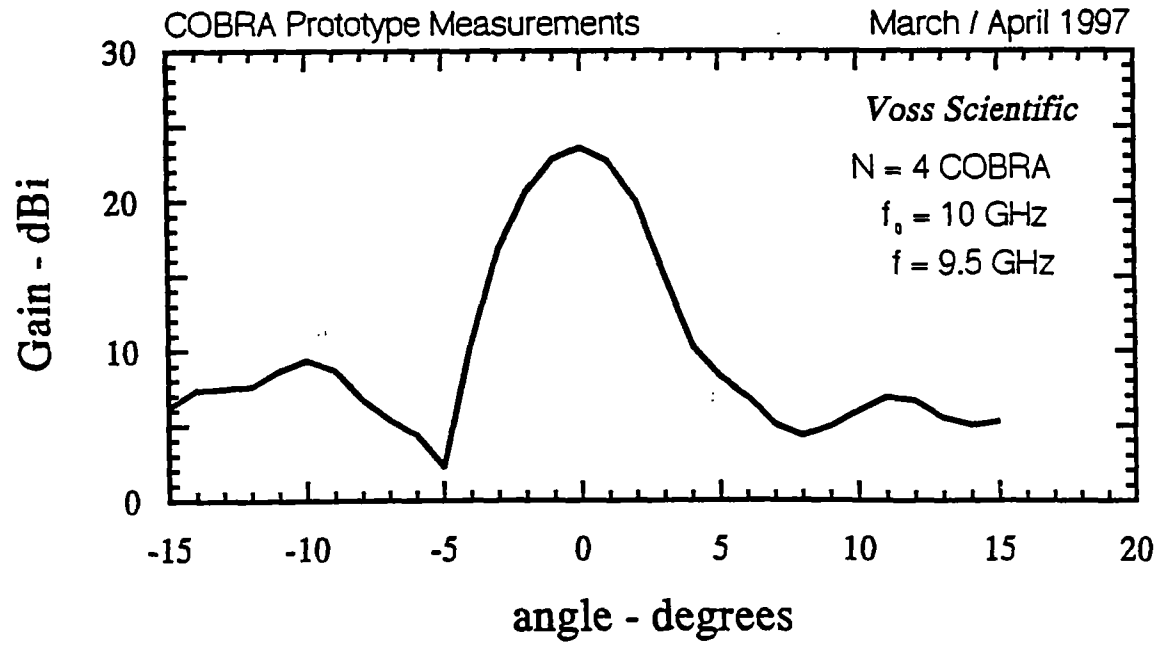

Figure 7-4 **Co-polarized pattern of the N=4 COBRA prototype in the azimuthal plane. The measurement frequency was 9.5 GHz.**

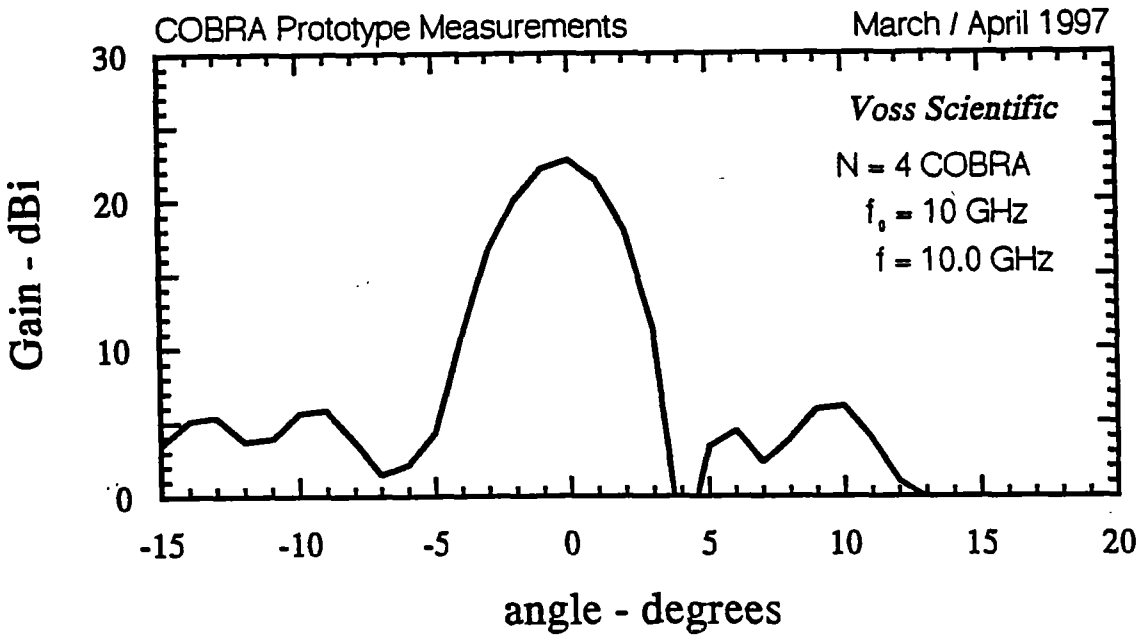

Figure 7-5 **Co-polarized pattern of the N=4 COBRA prototype in the azimuthal plane. The measurement frequency was 10 GHz.**

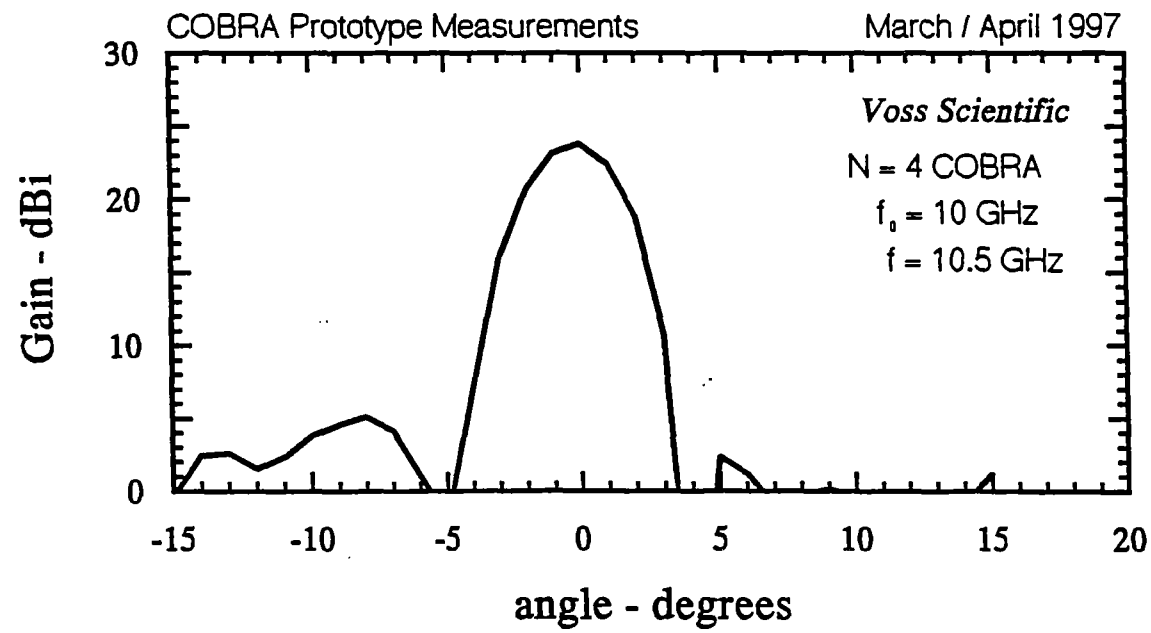

Figure 7-6 **Co-polarized pattern of the N=4 COBRA prototype in the azimuthal plane. The measurement frequency was 10.5 GHz.**

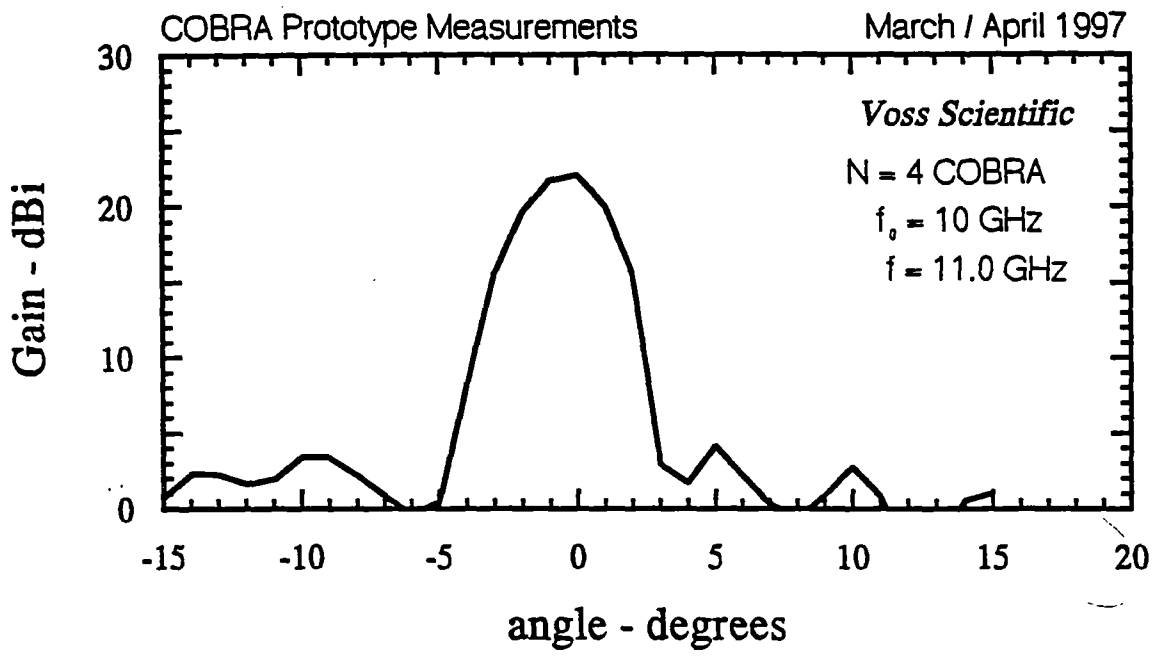

Figure 7-7 **Co-polarized pattern of the N=4 COBRA prototype in the azimuthal plane. The measurement frequency was 11 GHz.**

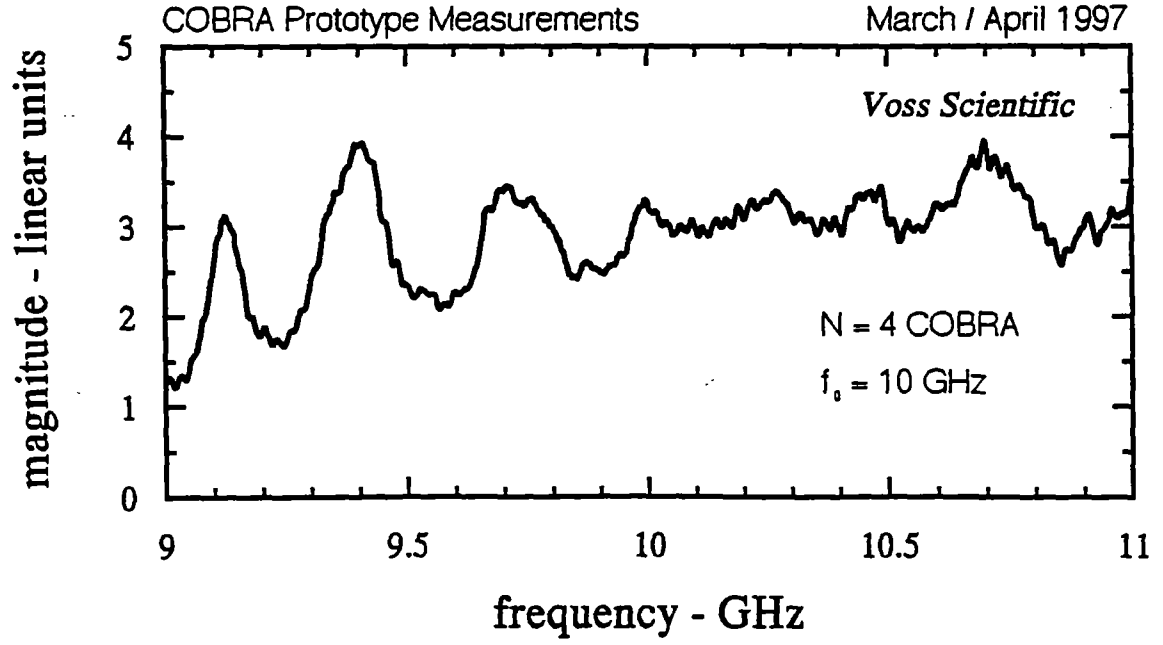

Figure 7-8 **Relative magnitude of the horizontal polarized component of the boresight field of the N=4 COBRA as a function of frequency.**

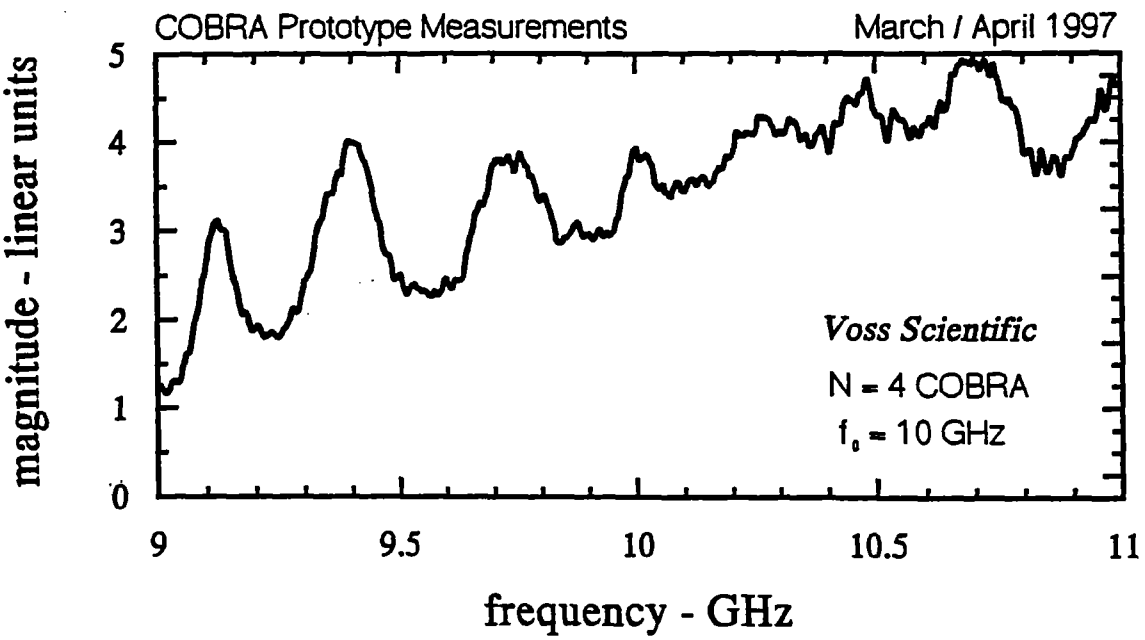

Figure 7-9 **Relative magnitude of the vertical polarized component of the boresight field of the N=4 COBRA as a function of frequency.**

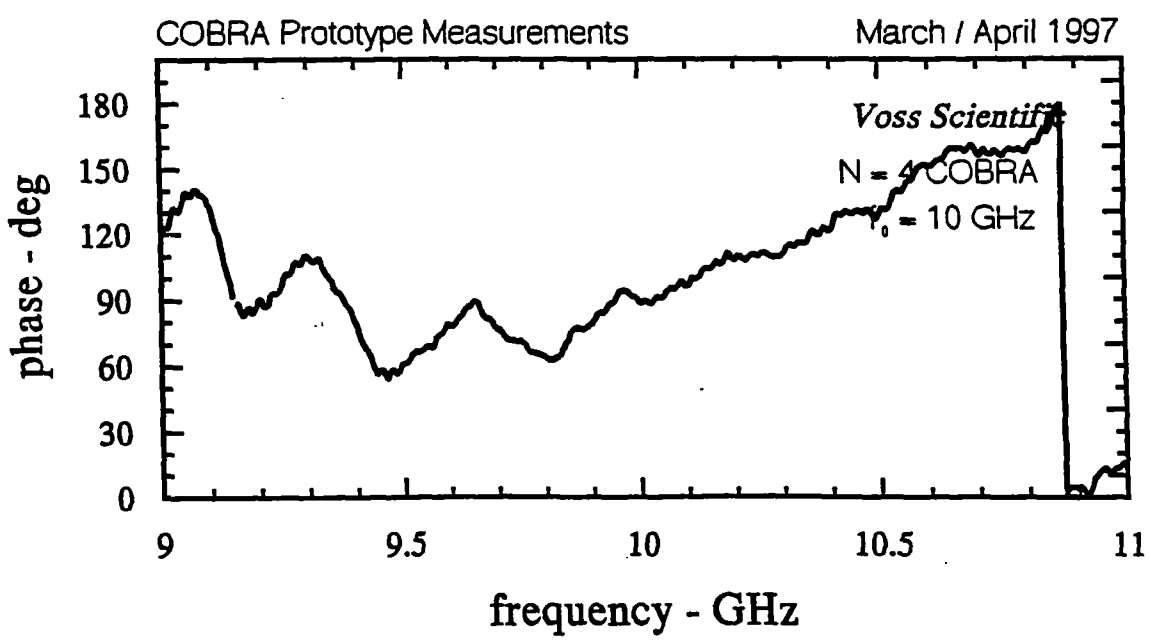

Figure 7-10 **Relative phase of the horizontal polarized component of the boresight field of the N=4 COBRA as a function of frequency.**

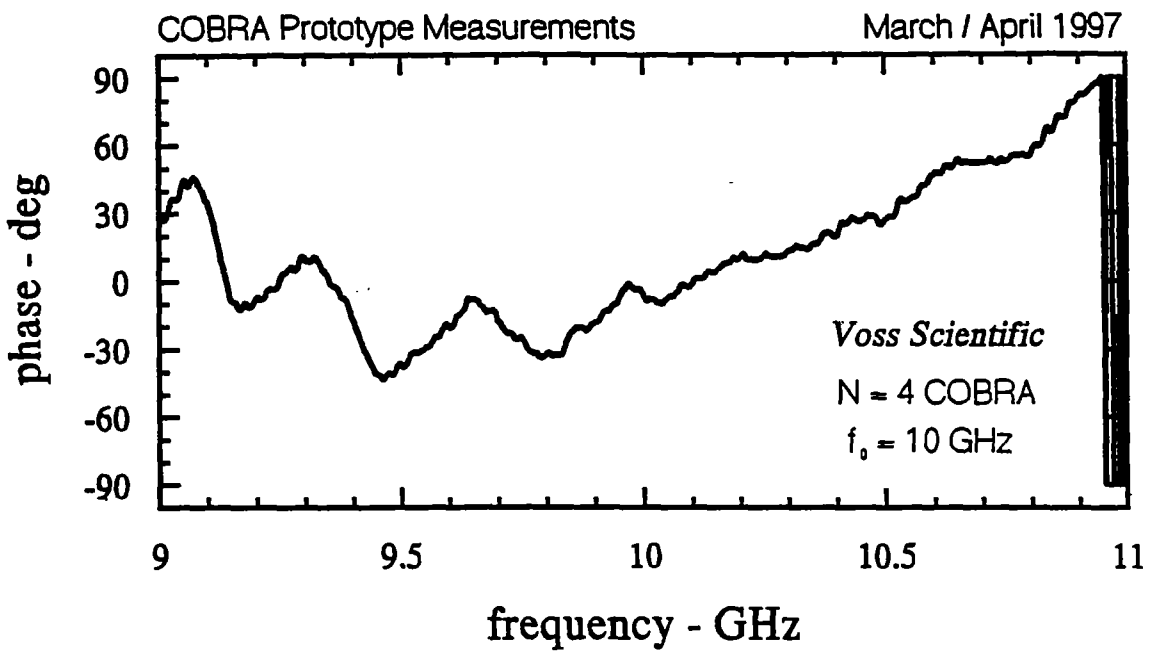

Figure 7-11 Relative phase of the vertical polarized component of the boresight field of the N=4 COBRA as a function of frequency.

8. SUMMARY, OBSERVATIONS AND CONCLUSIONS

These measurements were conducted to provide insight into the operating properties and bandwidth of N=1, N=2 and N=4 COBRA configurations. Absolute gain and pattern, and relative boresight measurements were made for numerous different configurations. This section consolidates the many results presented in the previous section, and provides a metric (aperture efficiency) by which to judge the COBRA prototype's overall efficiency and performance. This section closes with some general observations, and a list of measurements that should have been made. Such is the nature of hindsight.

8.1 Physical Aperture of the COBRA Prototype

The COBRA antenna's normalized (to wavelength) physical aperture is defined by the diameter of the parabolic reflector and the operating frequency. The maximum gain of a uniformly illuminated aperture is

$$G_{\max} = \frac{4\pi}{\lambda^2} Area \text{, which in this case is } G_{\max} = \frac{4\pi}{\lambda^2}\left(\pi\left(\frac{0.6096}{2}\right)^2\right) = \frac{3.67}{\lambda^2} = 10\log\left[\frac{3.67}{\lambda^2}\right] \text{ dB.}$$

The maximum gain as a function of frequency is presented in Table 8-1. The gain of an antenna can be expressed in terms of its effective aperture area as in

$$G = \frac{4\pi}{\lambda^2} A_e \text{ , or } A_e = G\frac{\lambda^2}{4\pi}.$$

The aperture efficiency then is simply $\varepsilon_{ap} = A_e / A_p$ [3].

Table 8-1 Physical aperture gain of the 24-inch COBRA parabolic reflector.

frequency GHz	Numerical Maximum Gain	Maximum Gain dBi
9	3,303	35.2
9.5	3,680	35.7
10	4,077	36.1
10.5	4,495	36.5
11	4,934	36.9

8.2 Performance Summary of the COBRA Prototype

This section provides a "quick look" at the measurement results. Only the measurements made of the COBRA and the COBRA feed horn are included in Table 8-2. The following information is given on each line of the table: (1) antenna type, (2) "N" number, (3) boresight characteristic (peak or null), (4) boresight polarization (linear, cross-polarized, circular), (5) scanplane (azimuth or elevation), (6) maximum gain, (7) pattern sidelobe level, (8) aperture efficiency, and (9) the related figure in the body of the report (typically a measured pattern). All of the results reported in Table 8-2 are for a 10 GHz center frequency.

Table 8-2 Performance summary for the COBRA prototype measurements.

Antenna	N	Boresight Peak/Null	Boresight Polarization	Scan plane	Max Gain dBi	SLL dBi	ε_{ap}	Figure
Feed horn	×	null	×	az	3	×	×	Figure 4-3
COBRA	1	null	×	az	25	×	×	Figure 5-2
COBRA	2	peak	linear	az	26.8	6	.103	Figure 6-2
COBRA	2	null	x-polarized	az	17	×	×	Figure 6-1
COBRA	2	peak	linear	el	26.2	20	.102	Figure 6-8
COBRA	4	peak	circular	az	23.1 (d_L)	6	.05	Figure 7-2
COBRA	4	peak	circular	el	23.5 (d_L)	18	.055	Figure 7-1
COBRA	4	peak	circular		26.3 (d_C)		.105	

8.3 Conclusions and Observations

For the most part, the measurements yielded results as expected. The following general observations are noted.

The bandwidth of the different COBRA configurations is wider than expected. The feed horn or feed structure seems to be the bandwidth limitation in a COBRA system.

The aperture efficiency of the COBRA prototype was small (10% or less), meaning a much greater optimization was possible. Aperture efficiencies of 20% - 30 % are neither uncommon nor unreasonable. The feed horn design and optimization would be the obvious place to increase the COBRA design's aperture efficiency. One could expect at least a 3-dB improvement in the boresight gain with the proper optimization.

The center frequency for these measurements was 10 GHz. All physical adjustments of the COBRA prototype sectors were made according to the governing equations and this center frequency. The feed horn was placed in a somewhat arbitrary (described earlier) but seemingly sensible manner. One would expect optimum performance at the design center frequency; however, in the frequency sweeps for both the N=2 (Table 6-2) and N=4 (Table 7-2) configurations, and the boresight polarization (Table 7-3) measurements, we found slightly more optimal performance at 9.5 GHz. This could be a feed horn focus problem, or some other issue not addressed.

The biggest "surprise" of the measurements is the difference in sidelobe levels associated with the principal scan planes. Symmetry was expected in these patterns. One would think that as $N \rightarrow \infty$, or the steps become a continuous contour, that symmetry must exist. It is

expected that, as the number of sectors increases, the differences between the sidelobe levels in the different principal planes will become smaller. Whether this means the sidelobe levels will drop to the low values (peak to sidelobe ratios of > 20 dB) or increase to the higher values (peak to sidelobe ratios of = 5 dB) is unclear.

9. REFERENCES

1. Clifton C. Courtney and Carl E. Baum, "Coaxial Beam-Rotating Antenna (COBRA) Concepts," Phillips Laboratory Sensor and Simulation Note 395, Phillips Laboratory, 1996

2. Chris Jerome, et al, "Software User's Manual: Narrow Band Continuous Wave RF Diagnostic and Data Reduction System," Voss Scientific Technical Document VS-509, November 1995.

3. W. Stutzman and G. Thiele, *Antenna Theory and Design*, John Wiley, New York, 1981.